A Role for Actin, Cdc1p, and Myo2p in the Inheritance of Late Golgi Elements in *Saccharomyces cerevisiae*

Olivia W. Rossanese, Catherine A. Reinke, Brooke J. Bevis, Adam T. Hammond, Irina B. Sears, James O'Connor, and Benjamin S. Glick

Department of Molecular Genetics and Cell Biology, The University of Chicago, Chicago, Illinois 60637

Abstract. In *Saccharomyces cerevisiae*, Golgi elements are present in the bud very early in the cell cycle. We have analyzed this Golgi inheritance process using fluorescence microscopy and genetics. In rapidly growing cells, late Golgi elements show an actin-dependent concentration at sites of polarized growth. Late Golgi elements are apparently transported into the bud along actin cables and are also retained in the bud by a mechanism that may involve actin. A visual screen for mutants defective in the inheritance of late Golgi elements yielded multiple alleles of *CDC1*. Mutations in *CDC1* severely depolarize the actin cytoskeleton, and these mutations prevent late Golgi elements from being retained in the bud. The efficient localization of late Golgi elements to the bud requires the type V myosin Myo2p, further suggesting that actin plays a role in Golgi inheritance. Surprisingly, early and late Golgi elements are inherited by different pathways, with early Golgi elements localizing to the bud in a Cdc1p- and Myo2p-independent manner. We propose that early Golgi elements arise from ER membranes that are present in the bud. These two pathways of Golgi inheritance in *S. cerevisiae* resemble Golgi inheritance pathways in vertebrate cells.

Key words: Golgi apparatus • endoplasmic reticulum • budding yeast • actins • myosin

Introduction

Eukaryotic cells partition each of their organelles during cell division. In budding yeasts such as *Saccharomyces cerevisiae*, organelles must be delivered to the emerging bud (Yaffe, 1991). During S phase in *S. cerevisiae*, vacuoles and mitochondria are transported into the nascent bud by actin-dependent mechanisms (Hill et al., 1996; Simon et al., 1997; Catlett and Weisman, 2000). The nuclear material then partitions between the mother and daughter cells in a process that requires microtubules (Hildebrandt and Hoyt, 2000). Little is known about the inheritance of the ER and the Golgi apparatus, except that both of these organelles are present in the bud early in S phase (Segev et al., 1988; Redding et al., 1991; Preuss et al., 1991, 1992). We have initiated a molecular genetic analysis of Golgi inheritance in *S. cerevisiae*.

Ongoing studies of vertebrate cells have yielded two paradigms for Golgi inheritance. One paradigm states that the vertebrate Golgi fuses with the ER during mitosis and then reemerges to generate new Golgi stacks (Thyberg and Moskalewski, 1998; Zaal et al., 1999). In *S. cerevisiae*, the analogous process would be the de novo formation of Golgi cisternae from ER membranes that are present in the bud. The other paradigm states that preexisting vertebrate Golgi fragments are partitioned between the two daughter cells during cytokinesis (Lowe et al., 1998). In *S. cerevisiae*, the analogous process would be the transfer of preexisting Golgi cisternae into the bud. These two postulated modes of Golgi inheritance are not mutually exclusive, either in vertebrate cells (Hammond and Glick, 2000a) or in budding yeasts.

The inheritance of the *S. cerevisiae* Golgi apparatus poses an interesting problem because this organelle does not assemble into stacks; instead, early and late cisternae are scattered throughout the cytoplasm (Segev et al., 1988; Franzusoff et al., 1991; Antebi and Fink, 1992; Preuss et al., 1992; Lussier et al., 1995). We have proposed that this unusual Golgi organization is due to a delocalized transitional ER (tER)[1] compartment (Rossanese et al., 1999). The tER produces coat protein (COP) II transport vesicles, and accumulating evidence suggests that COPII vesicles ultimately give rise to new Golgi cisternae, implying that the Golgi can be viewed as an outgrowth of the tER (Bannykh and Balch, 1997; Kuehn and Schekman, 1997; Glick and Malhotra, 1998; Pelham, 1998). In *S. cerevisiae*, the

Address correspondence to Benjamin S. Glick, Department of Molecular Genetics and Cell Biology, The University of Chicago, 920 East 58th St., Chicago, IL 60637. Tel.: (773) 702-5315. Fax: (773) 702-3172. E-mail: bsglick@midway.uchicago.edu

[1]*Abbreviations used in this paper:* COP, coat protein; DIC, differential interference contrast; EGFP, enhanced GFP; GFP, green fluorescent protein; LatA, latrunculin A; QSD, quasi-synthetic dextrose medium; tER, transitional ER.

entire ER apparently functions as tER (Rossanese et al., 1999), so new Golgi cisternae should form throughout the cytoplasm. Some of these new Golgi cisternae will form in the bud. Other Golgi cisternae that have been generated in the mother cell might subsequently be transferred into the bud. Our findings suggest that both of these mechanisms contribute to Golgi inheritance in *S. cerevisiae*.

Materials and Methods

Strains, Media, and Growth Conditions

Yeast strains used in this study are shown in Table I. Apart from Ypt1-A136D, all of these strains are derivatives of JK9-3d (Kunz et al., 1993). In the case of BGY104, the *leu2-3,112* allele was converted to wild-type *LEU2* by amplifying the wild-type *LEU2* gene by PCR and using the resulting DNA fragment to transform the strain to leucine prototrophy. Green fluorescent protein (GFP) constructs were made using an enhanced *GFP* gene (*EGFP*; CLONTECH Laboratories, Inc.). Strains in which the *SEC7* gene was replaced with *SEC7–GFP* were constructed as previously described (Séron et al., 1998). To obtain brighter fluorescence, additional strains were engineered, as described below, to express *SEC7* fused to three tandem copies of *GFP*. pEGFP-1 (CLONTECH Laboratories, Inc.) was mutagenized to replace the *GFP* stop codon with GGTCCGG, creating a BspEI site. This intermediate plasmid, termed pEGFP-B1, was digested with BspEI and NotI, and an AgeI–NotI fragment from pEGFP-1 was inserted to yield pEGFP-12, which contains two tandem copies of *GFP*. The double *GFP* cassette was excised from pEGFP-12 with AgeI and NotI and subcloned into pEGFP-B1, as described above, to yield pEGFP-13, which contains three tandem copies of *GFP*. Finally, the triple *GFP* cassette was excised from pEGFP-13 with BamHI and NotI and subcloned into pUSE-URA3 (Séron et al., 1998), which had been digested with BamHI and EagI. The resulting plasmid was linearized with SpeI for pop-in–pop-out replacement of *SEC7* with *SEC7–GFPx3* (Rothstein, 1991; Séron et al., 1998). Strains expressing *SEC13-GFP* were constructed as previously described (Rossanese et al., 1999).

Strains expressing *SEC21-GFPx3* were constructed as described below. A DNA fragment comprising the last 205 nucleotides of the *SEC21* gene plus 421 nucleotides downstream of the stop codon was amplified by PCR and was inserted into YIplac211 (Gietz and Sugino, 1988), which had been cut with PvuII. The QuikChange method (Stratagene) was used to replace the stop codon of *SEC21* with a BamHI–NotI cassette. Finally, the triple *GFP* cassette from pEGFP-13 was inserted as a BamHI–NotI fragment. The resulting construct was linearized with BclI for pop-in–pop-out replacement of *SEC21* with *SEC21-GFPx3*. A similar strategy was used to replace *RIC1* with *RIC1–GFPx3*, except that the final construct was linearized with PacI for integration. Strain BGY231, which expresses Mnt1p–Kre2p with a COOH-terminal triple myc tag (Jungmann and Munro, 1998), was also generated by a pop-in–pop-out gene replacement.

Strains expressing *GFP-YPT1* were constructed as described below. A BspHI site was introduced after the second codon of *YPT1* (sequence from start codon: ATGAATGTCATGAGCGAG). Meanwhile, pEGFP-C1 (CLONTECH Laboratories, Inc.) was mutagenized to introduce an NcoI site between the BglII and EcoRI sites in the polylinker (sequence: AGATCTGCCATGGGAATTC). The *GFP* gene was excised from the resulting plasmid with NcoI and was inserted at the BspHI site in the modified *YPT1* gene. Finally, a KpnI–BamHI fragment containing *GFP-YPT1* under control of the *YPT1* promoter was inserted into the corresponding sites in YIplac128 (Gietz and Sugino, 1988). The resulting plasmid was linearized with ClaI and integrated into the *LEU2* locus.

Strains containing GFP–HDEL in the ER lumen were constructed as described below. An EcoRV–HindIII fragment containing the *CYC1* transcription terminator (Osborne and Guarente, 1989) was inserted into YIplac204 (Gietz and Sugino, 1988), which had been cut with HincII and HindIII. The resulting plasmid was digested with EheI and SmaI, and a fusion (generated by overlap extension PCR; Ho et al., 1989) of the *TPI1* promoter to the first 135 nucleotides of the *KAR2* gene was inserted. Finally, the *GFP* gene was amplified by PCR and simultaneously modified to encode a COOH-terminal HDEL tetrapeptide, and this PCR fragment was inserted into the previous construct as a BamHI–XbaI fragment. The final construct encodes the Kar2p presequence joined to the NH_2 terminus of GFP–HDEL by the linker peptide ADDGDPPVAT. This plasmid was linearized with EcoRV and integrated into the *TRP1* locus.

Expression of ER-targeted GFP–HDEL did not significantly affect cell growth. The *GFP–YPT1* fusion gene is functional, as judged by its ability to rescue growth of the thermosensitive Ypt1–A136D strain at 37°C; however, GFP–Ypt1p sometimes had a clumpy appearance in slowly growing cells, suggesting that this fusion protein is subtly different from authentic Ypt1p. The *GFP* fusions with *SEC7*, *SEC13*, and *SEC21* are also functional, as judged by their ability to support normal growth in place of the cognate chromosomal genes. Previous work has established that GFP-tagged Ric1p is functional (Siniossoglou et al., 2000). In the case of Sec7p, Sec21p, and Ric1p, the single GFP–tagged versions seem to behave identically to the triple GFP–tagged versions with respect to protein localization and cell growth, indicating that these proteins tolerate the triple GFP tag.

Table I. Yeast Strains Used in This Study

Strain	Genotype	Reference
JK9-3dX	l*eu2-3,112 ura3-52 trp1 his4 rme1*	Kunz et al., 1993
BGY101	JK9-3d**a** *SEC7-GFP*	This study
BGY103	JK9-3d**a** *SEC7-GFP bar1::URA3*	This study
BGY104	JK9-3dα *SEC7-GFP LEU2*	This study
BGY316	JK9-3d**a** *SEC7-GFPx3*	This study
BGY418	JK9-3d**a** *TRP1::GFP-HDEL*	This study
BGY318	JK9-3d**a** *SEC13-GFP*	This study
BGY210	JK9-3d**a** *RIC1-GFPx3*	This study
BGY211	JK9-3d**a** *SEC21-GFPx3*	This study
BGY214	JK9-3d**a** *LEU2::GFP-YPT1*	This study
BGY108	JK9-3d**a** *cdc1-304*	This study
BGY105	JK9-3d**a** *cdc1-304 SEC7-GFP*	This study
BGY111	JK9-3d**a** *cdc1-304 SEC7-GFPx3*	This study
BGY419	JK9-3d**a** *cdc1-304 TRP1::GFP-HDEL*	This study
BGY110	JK9-3d**a** *cdc1-304 SEC13-GFP*	This study
BGY221	JK9-3d**a** *cdc1-304 RIC1-GFPx3*	This study
BGY225	JK9-3d**a** *cdc1-304 SEC21-GFPx3*	This study
BGY215	JK9-3d**a** *cdc1-304 LEU2::GFP-YPT1*	This study
BGY402	JK9-3d**a** *act1-ΔDSE*	This study
BGY414	JK9-3d**a** *act1-ΔDSE SEC7-GFPx3*	This study
BGY403	JK9-3d**a** *myo2-66*	This study
BGY415	JK9-3d**a** *myo2-66 SEC7-GFPx3*	This study
BGY420	JK9-3d**a** *myo2-66 TRP1::GFP-HDEL*	This study
BGY434	JK9-3d**a** *myo2-66 SEC13-GFP*	This study
BGY222	JK9-3d**a** *myo2-66 RIC1-GFPx3*	This study
BGY226	JK9-3d**a** *myo2-66 SEC21-GFPx3*	This study
BGY216	JK9-3d**a** *myo2-66 LEU2::GFP-YPT1*	This study
BGY231	JK9-3d**a** *MNT1-myc*	This study
Ypt1-A136D	*ura3-52 his4 ypt1-A136D*	Jedd et al., 1995

Only the most relevant strains are listed. To test the role of actin in Sec7p–GFP inheritance, *SEC7–GFP* was introduced into additional haploid strains containing the following actin alleles (Wertman et al., 1992): *ACT1, act1-101, act1-102, act1-104, act1-105, act1-108, act1-111, act1-112, act1-113, act1-115, act1-116, act1-117, act1-119, act1-120, act1-121, act1-122, act1-123, act1-124, act1-125, act1-129, act1-132, act1-133, act1-135,* and *act1-136*.

The *act1-ΔDSE* and *myo2-66* mutations were introduced into JK9-3d**a** by the pop-in–pop-out method (Rothstein, 1991). After the integrated plasmids had been popped out, the presence of the mutant alleles was confirmed by PCR amplification and sequencing of the relevant genomic DNA regions. To generate the *act1-ΔDSE* replacement construct, the *act1-ΔDSE* allele was excised from pCEN-ΔDSE (Cook et al., 1992) with AflIII, blunted with Klenow, and inserted into the Ecl136II site of pUC19-URA3 (Rossanese et al., 1999). The resulting plasmid was linearized with SspI for integration. To generate the *myo2-66* replacement construct, a DNA fragment containing a 3′ portion of the *myo2-66* allele (Johnston et al., 1991) was excised by digesting with ClaI, blunting with Klenow, and digesting with SalI; this fragment was then subcloned into pUC19-URA3, which had been digested with Ecl136II and SalI. The resulting plasmid was linearized with BamHI for integration.

Unless otherwise indicated, yeast strains to be viewed by fluorescence microscopy were grown in a minimally fluorescent quasi-synthetic dextrose medium (QSD) (0.67% yeast nitrogen base, 2% glucose, 0.01% $CaCl_2{\cdot}2H_2O$, 0.05% NaCl, 0.05% $MgCl_2{\cdot}6H_2O$, 0.1%NH_4Cl, 0.5% KH_2PO_4, 0.1% K_2HPO_4, 1X complete supplemental mixture [Bio101]). QSD yields very rapid growth and has a relatively low background fluorescence. Some experiments used rich medium (YPD) (1% yeast extract, 2% peptone, 2% glucose, 20 mg/liter adenine sulfate, 20 mg/liter uracil).

Antibodies

The following antibodies and concentrations were used for immunofluorescence. Mouse monoclonal anti–β-tubulin (clone KMX-1; Roche) was used at 1 μg/ml, and anti-GFP (a mixture from clones 7.1 and 13.1; Roche) was used at 5 μg/ml. Rabbit polyclonal anti-GFP (CLONTECH Laboratories, Inc.) was used at 1:200 dilution. Rabbit polyclonal anti-Sec7p (Franzusoff et al., 1991), affinity purified as described (Harlow and Lane, 1988) against a fusion protein comprising glutathione *S*-transferase linked to the NH_2-terminal acidic portion of Sec7p (Rossanese et al., 1999), was used at 1:100 dilution. Fluorescent secondary antibodies from donkey (Jackson ImmunoResearch Laboratories) were used at 1:200 dilution.

Viewing Intracellular Structures by Fluorescence Microscopy

Immunofluorescence microscopy of yeast was performed as previously described (Rossanese et al., 1999). Cells expressing a GFP fusion or cells that had been stained with FM4-64 (N-(3-triethylammoniumpropyl)-4-(6-(4-(diethylamino)phenyl)hexatrienyl) pyridinium dibromide; Molecular Probes) were incubated under the appropriate conditions and then fixed as described below. A 0.4-ml aliquot of a yeast culture was mixed with an equal volume of ice-cold 2X fixative (100 mM potassium phosphate, pH 6.5, 2 mM $MgCl_2$, 8% formaldehyde, 0.5% glutaraldehyde). After 1 h on ice in the dark, the cells were washed twice with 1 ml PBS and resuspended in 50 μl PBS. For viewing, 1.5 μl of the resuspended cells was placed on a glass slide and spread with a coverslip.

Vacuoles were labeled by the method of Hill et al. (1996). Cells were grown in QSD to an OD_{600} of 0.8–1.0, and a 0.25-ml aliquot of the culture was incubated for 1 h at room temperature in the dark with 80 μM FM4-64, diluted from a 3.3 mM stock solution in DMSO. The cells were washed three times with 1 ml QSD, diluted into 2–5 ml QSD, and allowed grow for an additional 2–4 h. Finally, the cells were resuspended in 0.1 ml QSD and fixed as above.

Actin was visualized as described below. A yeast culture was grown overnight with good aeration to an OD_{600} of 1, and fixed as above. After the final wash, the cells were resuspended in PBS, pH 7.4, 0.5% octyl glucoside, to an OD_{600} of 10. Then, 92.4 μl of cell suspension was transferred to a microfuge tube, and 7.6 μl of Alexa 594–phalloidin (6.6 μM in methanol; Molecular Probes) was added while vortexing, yielding a final Alexa 594–phalloidin concentration of 0.5 μM. The sample was mixed end-over-end for 1 h in the dark. Cells were washed three times with 200 μl cold PBS. After the final wash, the cells were resuspended in 10 μl phenylenediamine-containing mounting medium (Pringle et al., 1991). 1.5 μl of this suspension was mounted and viewed.

Fluorescence and differential interference contrast (DIC) imaging, photography, and image processing were carried out as previously described (Rossanese et al., 1999).

Treatment with α-Factor, Latrunculin A, and Nocodazole

Cells to be treated with α-factor were grown overnight in YPD at 30°C (or 23°C for thermosensitive mutants) to an OD_{600} of 0.8–1.0, centrifuged, and resuspended to the same OD_{600} in fresh YPD. α-Factor was added to a final concentration of 0.5 μM from a 1 mg/ml (594 μM) stock in DMSO, and the culture was incubated with shaking for 90 min. For treatment with latrunculin A (LatA) or nocodazole, cells were grown overnight in QSD to an OD_{600} of 1. Then a 400-μl aliquot was transferred to a microfuge tube, and 4 μl of either 20 mM LatA or 1.5 mg/ml nocodazole in DMSO (Molecular Probes) was added while vortexing to give a final concentration of 200 μM LatA or 15 μg/ml nocodazole. Control aliquots received an equal volume of DMSO. The cells were transferred to a 5-ml Falcon tube, returned to 30°C with shaking for 30 min, and then fixed and either stained with Alexa 594–phalloidin to visualize actin (see above) or processed for immunofluorescence using an antitubulin antibody (Rossanese et al., 1999). As previously reported, LatA caused a rapid depolymerization of actin cables and patches (Ayscough et al., 1997), whereas nocodazole caused a rapid depolymerization of microtubules (Jacobs et al., 1988).

Isolation of the Mutant Strains

Strain BGY103 was mutagenized to 3–5% survival by treatment with ethyl methanesulfonate (Lawrence, 1991). The following method was used for rapid identification of temperature-sensitive mutants. Mutagenized cells were plated on 150-mm-diam YPD plates and grown at 23°C to yield ~5,000 colonies per plate. Each plate was replica-plated onto a fresh YPD plate for growth at 37°C, and onto a second YPD plate for growth at 23°C. After a suitable growth period, the 37°C and 23°C plates were photocopied to yield images of white colonies on a black background. (This step was facilitated by using relatively thin YPD plates.) The image of the 37°C plate was scanned with a Hewlett-Packard ScanJet 4c scanner, using the DeskScan II software set to "sharp black and white drawing". This image was imported into Adobe® Photoshop™ and inverted, yielding an image of black colonies on a clear background. This inverted image was printed onto a transparency and overlaid on the photocopy of the 23°C plate. The black spots on the transparency obscured the underlying white spots, except in the case of clones that had failed to grow at 37°C. Colonies that appeared as white in this assay were subjected to a second round of testing, and ~70% turned out to be bona fide temperature-sensitive mutants. Using this procedure, we isolated 4,000 temperature-sensitive derivatives of BGY103.

These mutants were screened as described below for alterations in Golgi inheritance or morphology. Mutant clones were grown in QSD in 96-well plates, with shaking for 2 d at room temperature. The cultures were then diluted 1:1 into fresh QSD, grown at room temperature for an additional 4–6 h, and shifted to 37°C for 2 h before viewing. A ceramic benchtop 96-well plate warmer (Thermolyne) was used to maintain the samples at 37°C during the viewing process, and a second plate warmer was used to prewarm the microscope slides. From each well in the plate, 1.5 μl was pipetted onto a prewarmed slide and spread with a 22-mm glass coverslip. Cells were viewed by fluorescence and DIC microscopy to evaluate Golgi inheritance and morphology. Using this visual screen, we typically examined two 96-well plates per day. Mutants with interesting Golgi patterns were subjected to additional rounds of screening, and those that displayed reproducible phenotypes were chosen for further analysis.

Quantitation of Organellar Inheritance

To quantify the rates of organellar inheritance, randomly chosen fields of cells were photographed in both DIC and fluorescence modes. A single DIC image was captured while fluorescence images were collected as a stack and then deconvolved and projected (Rossanese et al., 1999). Analyses were performed with Adobe® Photoshop™ and NIH Image (National Institutes of Health). Using the DIC images, all of the visibly budded cells were chosen, and each cell was assigned to one of five bud size categories based on the cross-sectional area of the bud, as measured with NIH Image. Category I buds had cross-sectional areas between 4.0 and 7.4% of the average cross-sectional area of the mother cells. The corresponding percentages for the other bud size categories were as follows: category II, 7.5–10.9%; category III, 11.0–14.4%; category IV, 14.5–17.9%; category V, 18.0–21.4%. Assuming that the cells were spherical, the bud volumes as a percentage of the average mother cell volume can be estimated as follows: category I, 0.8–2.0%; category II, 2.1–3.6%; category III, 3.7–5.5%; category IV, 5.5–7.6%; category V, 7.6–9.9%. The examination of budded cells was continued until 20 cells had been identified for each bud size category. The corresponding fluorescence images were then examined with Photoshop™, and each bud was scored for the presence or absence of fluorescent structures. For each of the plots in the figures, two separate experiments were performed, and the numbers were combined. Unless otherwise indicated, the different curves in a given plot compare cultures that were incubated under identical growth conditions.

Cloning of CDC1

The gene that is defective in the class A mutants was cloned by backcrossing one of these mutant strains four times to the parental strain (using BGY104 for the first backcross) to yield strain BGY105, and then transforming BGY105 with a *URA3 CEN* yeast genomic DNA library (a gift of Mark Hochstrasser (Yale University, New Haven, CT); Rose et al., 1987) and selecting for restoration of growth at 37°C. Fluorescence microscopy confirmed that the complementing plasmids also restored normal Sec7p–GFP inheritance. Sequencing and subcloning showed that the complementing gene was *CDC1*. Therefore, the backcrossed mutant strain was designated *cdc1-304*. We used two approaches to confirm that *CDC1* is the relevant gene. First, genomic DNA samples from the parental and *cdc1-304* strains were used for PCR amplification of the corresponding *CDC1* alleles, which were cloned into plasmid YCplac33 (Gietz and Sugino, 1988). The wild-type *CDC1* allele complemented the high temperature growth defect of the mutant strain, whereas the *cdc1-304* allele showed no complementation. Second, *CDC1* is only ~25 kb from *SEC7* on chromosome IV, implying that the mutations in the class A strains should be tightly linked to the *SEC7–GFP* marker. To test this prediction, a *cdc1-304 SEC7–GFP* strain was mated with a *CDC1 SEC7* strain, and the resulting diploid was sporulated. As expected, most of the tetrads failed to segregate the temperature-sensitive growth phenotype away from the fluorescence conferred by *SEC7–GFP*.

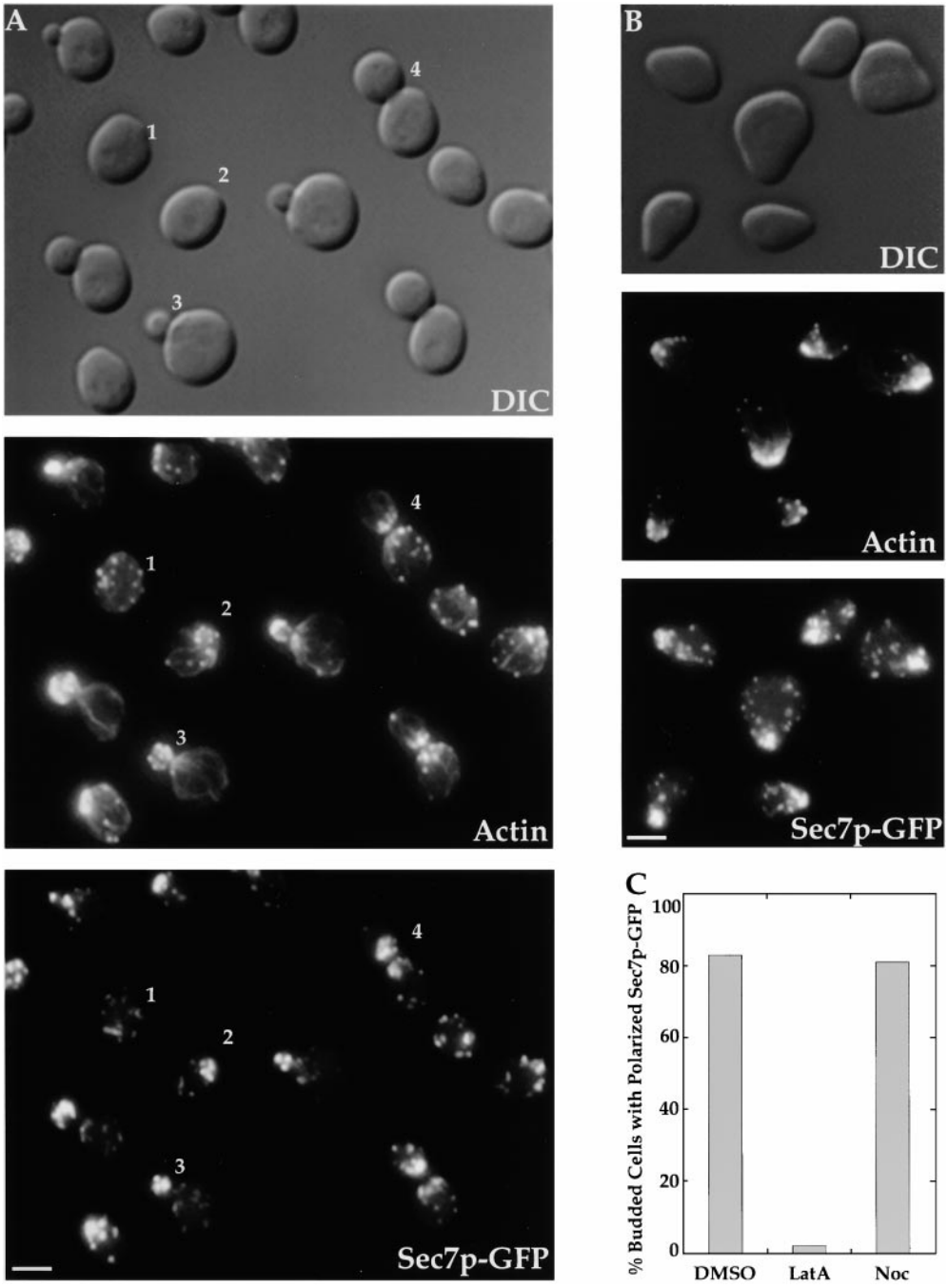

Figure 1. Sec7p–GFP is concentrated at sites of polarized growth in rapidly growing or schmooing cells. (A) Visualization of actin and Sec7p–GFP through the cell cycle. An unsynchronized culture of BGY316 cells growing rapidly at 30°C was fixed and stained with Alexa 594–phalloidin. The cells were then imaged by DIC microscopy and dual-color fluorescence microscopy. Numbers mark examples of a nonpolarized G1 cell (1), a polarized G1 cell (2), an S phase cell (3), and a cell undergoing cytokinesis (4). Actin patches and Sec7p–GFP are both concentrated at sites of polarized growth. (B) Distributions of actin and Sec7p–GFP in schmooing cells. A BGY316 culture was treated with α-factor for 90 min at 30°C, and then fixed and viewed as in A. Actin patches and Sec7p–GFP are concentrated in the schmoo. (C) Effects of disrupting actin or microtubules on the Sec7p–GFP pattern in rapidly growing cells. Aliquots of a rapidly growing BGY316 culture were either left untreated (DMSO), or treated with 200 μM LatA or 15 μg/ml nocodazole (Noc) for 30 min at 30°C before fixation. A portion of each aliquot was stained with Alexa 594–phalloidin to confirm that actin polymers had been disrupted by LatA, and a second portion was processed for immunofluorescence to confirm that microtubules had been disrupted by nocodazole (not shown). 50 budded cells from each aliquot were examined as in A, and the results from two separate experiments were combined. A cell was scored as having polarized Sec7p–GFP if it displayed a clear concentration of fluorescence in or near the bud. As judged by this assay, the polarization of Sec7p–GFP is effectively abolished by LatA treatment but is unaffected by nocodazole treatment. Bars, 2 μm.

Confocal Microscopy of Living Cells

Cells of strain BGY316 or BGY111 were grown in QSD at room temperature to an OD_{600} of ~0.5. To immobilize the cells for imaging, a ΔT dish (Bioptechs) was pretreated with a 2 mg/ml solution of concanavalin A (Sigma-Aldrich), allowed to dry, and washed with distilled water. An aliquot of the culture was added to the dish and left undisturbed for 30 min. Unbound cells were then removed by gentle washing. For imaging, the immobilized cells were gradually shifted to 37°C over a period of 20 min and were held at 37°C for an additional 1.5–2 h. Temperature control was achieved using Bioptechs ΔT and objective controllers. Single cells were imaged repeatedly with a 100X 1.4-NA PlanApo objective and a ZEISS Axiovert microscope, equipped with an LSM 510 confocal scanner. A piezoelectric objective controller was used to drive continuous objective movement, thereby allowing for the rapid collection of four-dimensional data sets (Hammond and Glick, 2000b). The GFP signal was visualized by excitation with a 488-nm laser and collection with a 505-nm longpass filter. Complete *z*-stacks were captured at intervals of 2.5 s, with the pinhole adjusted to yield 1.2 Airy units and a *z*-axis spacing of 0.35 μm between optical sections. Transmitted light images of the cells were collected simultaneously. The fluorescence images were processed with a 3 × 3 hybrid median filter to remove shot noise and then were projected using an average intensity algorithm that included multiplying the pixel values by an appropriate scaling factor to provide adequate contrast (Hammond and Glick, 2000b). Transmitted light images were projected using a maximum intensity algorithm. These filtering and projection operations were performed using custom macros written in NIH Image. The projected fluorescence and transmitted light images were merged using Adobe® Photoshop™.

Results

Analyzing Golgi Inheritance in S. cerevisiae

To visualize the Golgi in *S. cerevisiae*, we have fused GFP to proteins that are associated with the cytosolic face of Golgi membranes. This strategy was chosen because GFP folds more efficiently in the cytosol than in the lumen of the yeast secretory pathway (Wooding and Pelham, 1998). GFP can be linked to the cytosolic portions of integral Golgi membrane proteins (Wooding and Pelham, 1998), but such constructs often yield a background ER fluorescence under suboptimal growth conditions (not shown). Therefore, we used peripherally associated Golgi membrane proteins. For most of our experiments, the *SEC7* gene was replaced with a *SEC7–GFP* fusion gene (Séron et al., 1998). Sec7p is an abundant peripheral membrane protein of the late Golgi complex (Franzusoff et al., 1991), and, in a typical cell, Sec7p–GFP labels ~10–15 cytoplasmic spots that apparently correspond to individual Golgi cisternae (Preuss et al., 1992; Séron et al., 1998).

The first question that arose was: how should we define Golgi inheritance? In studies of mitochondria and vacuoles, inheritance has been defined as the transfer of preexisting organellar material from the mother cell into the bud (Yaffe, 1991; Catlett and Weisman, 2000). However, mitochondria and vacuoles are long-lived entities, whereas yeast Golgi cisternae are probably transitory structures with a lifetime of only a few minutes (Wooding and Pelham, 1998; Morin-Ganet et al., 2000). As described in the Introduction, Golgi cisternae might localize to the bud either by the transfer of preexisting cisternae or by de novo formation. These practical and theoretical considerations led us to define Golgi inheritance as the presence of Golgi elements in the bud. The amount of Golgi material in the bud varies widely under different growth conditions, but almost every bud contains some Golgi elements under all growth conditions (see below). Thus, for quantitative studies, we chose to assay simply for the presence or absence of a fluorescent Golgi marker in the bud.

Actin-dependent Concentration of Sec7p–GFP at Sites of Polarized Growth

Sec7p–GFP has previously been visualized as a set of spots distributed essentially evenly throughout the mother and daughter cells (Séron et al., 1998). However, Preuss et al. (1992) reported in an electron microscopy study that Golgi cisternae are clustered at the incipient bud site, within the bud, and at sites of cell wall synthesis during cytokinesis. This variability in the distribution of Golgi elements apparently reflects the growth state of the cells. Under many growth conditions, Sec7p–GFP shows little or no polarization; but in cultures that are growing very rapidly, Sec7p–GFP is clearly polarized (Fig. 1 A, bottom).

The Sec7p–GFP pattern in rapidly growing cells is reminiscent of the distribution of actin patches, which mark sites of polarized growth (Ayscough and Drubin, 1996; Botstein et al., 1997). Therefore, we used fluorescence microscopy to compare the locations of actin and Sec7p–GFP (Fig. 1 A, middle and bottom). The numbers 1–4 indicate cells at different stages of the cell cycle (Lew et al., 1997). In early G1 cells (1), neither actin nor Sec7p–GFP shows detectable polarization. In late G1 cells (2), actin patches and Sec7p–GFP are both concentrated at the incipient bud site. As actin patches move into the bud during S phase (3), Sec7p–GFP becomes concentrated in the bud. When actin patches repolarize to the sites of cytokinesis (4), Sec7p–GFP is also concentrated at these sites. Although the fluorescence patterns of actin patches and Sec7p–GFP do not actually overlap, these two patterns are similar throughout the cell cycle, confirming that late Golgi elements preferentially localize to sites of polarized growth.

An alternative way to induce Sec7p–GFP polarization is to expose haploid *MAT***a** cells to the pheromone α-factor (Sprague and Thorner, 1992). This treatment arrests the cell cycle in G1 and induces the formation of a mating projection, or schmoo. In α-factor–treated cells, Sec7p–GFP is almost always concentrated near the schmoo tip (Fig. 1 B). This result fits with an electron microscopy study that reported a clustering of Golgi cisternae in the schmoo (Baba et al., 1989). Thus, Sec7p–GFP is concentrated at sites of polarized growth in rapidly growing or schmooing cells.

One possible interpretation of these data is that late Golgi elements are transported along actin cables to sites of polarized growth. If so, then disrupting the actin cytoskeleton should abolish the polarization of Sec7p–GFP. To test this prediction, we treated a rapidly growing culture with LatA to block actin polymerization (Ayscough et al., 1997). LatA treatment disrupts dynamic actin structures, including cables and patches. In a mock-treated culture, ~80% of the budded cells showed clustering of Sec7p–GFP in or near the bud, whereas in the LatA-treated culture, <5% of the budded cells showed clustering of Sec7p–GFP (Fig. 1 C). As a control, when the culture was treated with nocodazole to depolymerize microtubules (Jacobs et al., 1988), Sec7p–GFP remained polarized (Fig. 1 C). This result matches our prediction. However, it should be noted that the LatA approach has two caveats. First, LatA-treated cells often abandon their current bud and choose a different bud site (Ayscough et al., 1997). Therefore, the loss of Sec7p–GFP polarization might reflect a general loss of cellular polarity cues. Second, cells that are growing suboptimally exhibit reduced polarization of Sec7p–GFP (see above), so LatA treatment might indirectly depolarize Sec7p–GFP by inhibiting cell growth. Despite these qualifications, our results support the idea that late Golgi elements undergo actin-dependent transport to sites of polarized growth.

LatA-resistant Localization of Sec7p–GFP to the Bud

Our goal is to understand how Golgi structures are incorporated into the newly formed bud. Initially, the most appealing idea was that late Golgi elements localize to the bud solely because of actin-dependent transport to sites of polarized growth. As predicted by this model, cells treated with LatA exhibit reduced Sec7p–GFP fluorescence in the bud (Fig. 2 A). A further prediction is that the Golgi elements in LatA-treated cells should be distributed randomly in the cytoplasm so that many of the small buds (i.e., those with volumes <10% of the average mother cell volume) should be devoid of Sec7p–GFP. For example, if the bud volume is 2% of the mother cell volume, and if the cell contains 15 randomly distributed fluorescent Golgi elements, then the probability that the bud contains one or

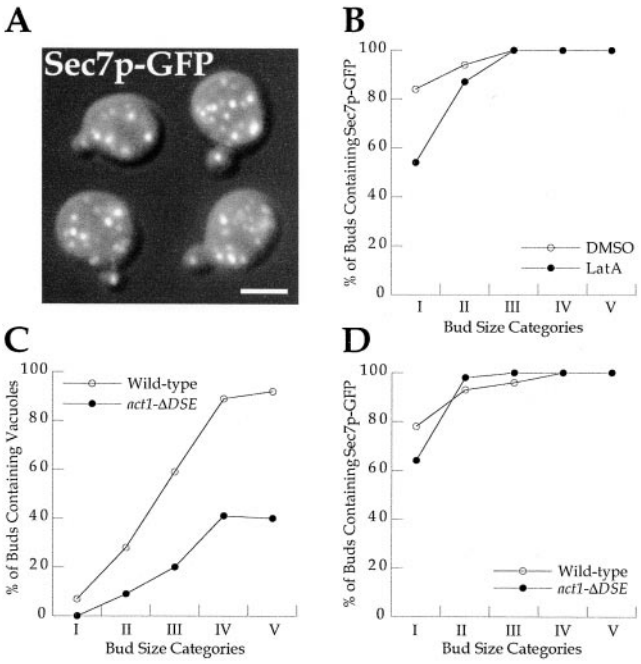

Figure 2. A subset of the late Golgi elements localize to the bud even after LatA treatment. (A and B) As described in the legend to Fig. 1 C, a rapidly growing BGY316 culture was treated with LatA for 30 min before fixation. Merged DIC and fluorescence images of representative LatA-treated cells are shown in A. Sec7p–GFP is generally depolarized, yet most of the small buds contain at least one spot of Sec7p–GFP fluorescence. This residual Sec7p–GFP inheritance is quantified in B. As described in Materials and Methods, budded cells from cultures mock treated with DMSO (○) or treated with LatA (●) were assigned to five categories on the basis of bud size, with category I cells having the smallest buds and category V the largest. Each budded cell was scored in a plus–minus manner for the presence of Sec7p–GFP in the bud. The results indicate that LatA treatment causes only a minor reduction in the percentage of buds containing Sec7p–GFP. (C and D) Cultures carrying the wild-type *ACT1* gene (strain BGY316; ○) or the *act1-ΔDSE* allele (strain BGY414; ●) were grown at 30°C, labeled with FM4-64, and fixed. Using the plus–minus visual assay, budded cells were assessed for the inheritance of vacuoles (C) and Sec7p–GFP (D). The *act1-ΔDSE* mutation inhibits vacuolar inheritance but has no effect on Sec7p–GFP inheritance. Bar, 2 μm.

more fluorescent Golgi elements is only ~25%. Surprisingly, however, most of the budded cells in a LatA-treated culture contain at least one spot of Sec7p–GFP fluorescence in the bud (Fig. 2 A). To quantify this effect, budded cells were scored using a plus–minus assay for the presence of Sec7p–GFP fluorescence in the bud. Under normal growth conditions (Fig. 2 B, ○), Sec7p–GFP is inherited very early, with ~70–90% of the nascent buds containing Sec7p–GFP by the time the bud volume reaches 0.8–2.0% of the average mother cell volume (category I). When the bud volume reaches 3.7–5.5% of the average mother cell volume (category III), essentially all of the buds contain Sec7p–GFP. Treatment with LatA (Fig. 2 B, ●) reduces the percentage of category I buds that contain Sec7p–GFP, but otherwise the numbers for control and LatA-treated cells are indistinguishable. For all of the bud size categories, the percentage of the buds that contain Sec7p–GFP after LatA treatment is much higher than predicted for a random distribution. This result indicates that a LatA-resistant mechanism localizes a subset of the late Golgi elements to the bud.

One limitation of these LatA experiments is that severe disruption of the actin cytoskeleton blocks bud formation, restricting the analysis to buds that were present before addition of the drug (Ayscough et al., 1997; Botstein et al., 1997). A gentler approach is to compromise actin function while still allowing the cells to grow in a polarized manner. For example, ΔDSE actin lacks the three residues that follow the initiator methionine (Cook et al., 1992), and *act1-ΔDSE* cells grow at essentially wild-type rates but have defects in myosin-driven transport (Cook et al., 1992; Hill et al., 1996). Rather than using an existing *act1-ΔDSE* strain, we introduced the *act1-DDSE* allele into our standard genetic background (Table I) because we find that different laboratory strains inherit various organelles at different stages of bud development. It was previously reported that *act1-ΔDSE* cells are strongly defective in vacuolar inheritance (Hill et al., 1996). We could readily verify this result. In our wild-type strain (Fig. 2 C, ○), vacuoles are inherited later than are the Golgi elements, but nearly all of the buds contain maternally derived vacuolar material by the time the buds reach 7.6–9.9% of the mother cell volume (category V). In cells carrying the *act1-ΔDSE* allele (Fig. 2 C, ●), vacuolar inheritance is dramatically inhibited. By contrast, *ACT1* and *act1-ΔDSE* cells are similar with regard to the percentage of buds that contain Sec7p–GFP (Fig. 2 D). To extend this analysis, we introduced *SEC7–GFP* into a set of yeast strains in which various charged-to-alanine codon substitutions had been made in the *ACT1* gene (Wertman et al., 1992). Many of these *act1* strains exhibit defects in the morphology and inheritance of vacuoles and mitochondria (Drubin et al., 1993; Smith et al., 1995; Hill et al., 1996); but as judged by our plus–minus visual assay, each of the *act1* mutants efficiently localizes Sec7p–GFP to the bud (not shown). Thus, a variety of conditions that are routinely used to disrupt the actin cytoskeleton do not block Sec7p–GFP inheritance.

These findings demonstrate that an intact actin cytoskeleton is not essential for inheriting the late Golgi complex. One possible interpretation is that an actin-independent process localizes a subset of the late Golgi elements to the bud. However, it is also possible that LatA-treated cells and *act1* mutant cells still contain residual actin structures in the bud, and that this residual bud-localized actin is required for efficient Golgi inheritance. As described below, our combined data favor this second possibility.

Isolation of Mutants with Altered Golgi Inheritance

To gain molecular insights into Golgi inheritance, we decided to take a genetic approach. The first step was to generate mutant derivatives of a strain expressing Sec7p–GFP. Because Golgi inheritance is presumably essential for viability, our analysis focused on mutants that were temperature sensitive for growth. 4,000 temperature-sensitive mutants were collected using a rapid screening procedure (Materials and Methods). Each of these mutants was grown at the permissive temperature, shifted briefly to 37°C, and viewed by DIC and fluorescence microscopy to ascertain whether Sec7p–GFP was present in the small buds.

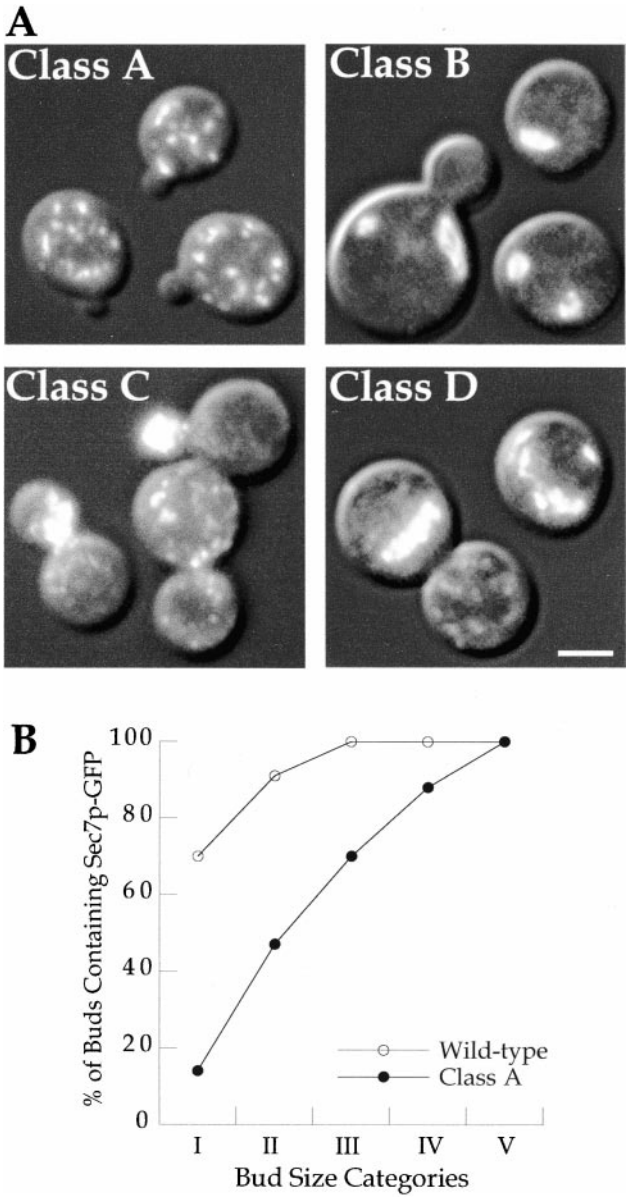

Figure 3. Mutants with altered inheritance or morphology of Sec7p–GFP-labeled Golgi elements. Cultures were grown overnight at room temperature and then shifted to 37°C for 1 h before fixation. (A) Golgi distribution and morphology in the four classes of mutants. DIC and fluorescence images were captured separately and merged. In class A mutants, the Sec7p–GFP-labeled Golgi elements exhibit normal size and distribution within the mother cell, but are frequently absent from the small buds. Strain BGY105 is shown. Class B mutants contain larger, fewer Golgi elements than wild-type cells. A typical class B cell has one to three large spots of Sec7p–GFP fluorescence. In class C mutants, the Golgi elements are smaller and more numerous than in wild-type cells. Moreover, class C mutants often display an even stronger polarization of late Golgi elements than do wild-type cells. The single class D mutant has a variety of Golgi morphology defects: Sec7p–GFP fluorescence can appear as rings, bars, or thin lines. (B) Cultures of wild-type cells (strain BGY316; ○) and a representative class A mutant (strain BGY111; ●) were grown at room temperature and then shifted to 37°C for 1 h before fixation. Quantitation by the plus–minus visual assay confirmed that Sec7p–GFP inheritance is defective in the class A mutant. Bar, 2 μm.

We identified 14 mutants that have normal patterns of Sec7p–GFP fluorescence in the mother cell but frequently lack Sec7p–GFP in the small buds. These Golgi inheritance mutants were designated class A (Fig. 3 A). The class A mutants all carry recessive single gene mutations, and they fall into a single complementation group. Therefore, we focused on a class A mutant that consistently showed a strong phenotype and backcrossed this mutant to the parental strain to transfer the mutation into a clean genetic background. Fig. 3 B shows a quantitation of the Golgi inheritance defect in this representative class A mutant. In wild-type cells, Sec7p–GFP is present in ~70% of the category I buds and in essentially all of the category III buds. In the class A mutant, Sec7p–GFP is present in only ~15% of the category I buds and ~70% of the category III buds. Only when the class A buds reach 7.6–9.9% of the average mother cell volume (category V) do virtually all of the buds contain Sec7p–GFP. Therefore, the class A mutants define a genetic locus that is essential for normal Golgi inheritance.

During the course of this screen for Golgi inheritance mutants, we also identified three classes of mutants with abnormal patterns of Sec7p–GFP fluorescence (Fig. 3 A). Class B mutants contain only one or a few large Sec7p–GFP-labeled Golgi elements per cell. The buds of class B mutants often lack Sec7p–GFP, but this inheritance defect is probably a secondary consequence of the altered Golgi structure. All six of the class B strains carry single gene recessive mutations, and these mutants fall into a single complementation group. In class C mutants, the Sec7p–GFP-labeled Golgi elements are smaller and more numerous than in the wild type. Moreover, class C mutants display an exaggerated form of the Sec7p–GFP polarization that is sometimes observed in wild-type cells (Fig. 1 A). We isolated 15 class C mutants, which fall into multiple complementation groups; genetic characterization of these strains is in progress. In the single class D mutant, the Sec7p–GFP-labeled Golgi elements display a variety of unusual shapes. Tetrad analysis revealed that the abnormal Golgi phenotype of class D cells is the result of a single recessive mutation that does not cosegregate with the temperature sensitivity phenotype. Although the class B, C, and D mutants are not specifically defective in Golgi inheritance, they will likely be useful for understanding the mechanisms that control Golgi distribution.

The Class A Phenotype Results from Mutations in CDC1

To identify the genetic locus that is mutated in class A cells, we isolated plasmids that rescue both growth and Sec7p–GFP inheritance at 37°C. Sequencing and subcloning revealed that the complementing DNA fragment is the *CDC1* gene (Halbrook and Hoekstra, 1994), and additional experiments confirmed that the defective Sec7p–GFP inheritance of class A mutants is due to alterations in *CDC1* (Materials and Methods). The *cdc1* allele in the representative class A mutant of Fig. 3 was designated *cdc1-304.* This allele contains a single base change that converts the codon for histidine-323 (CAC) to an asparagine codon (AAC).

cdc1 mutants were originally isolated as temperature-sensitive strains that arrested with small buds, 2N DNA,

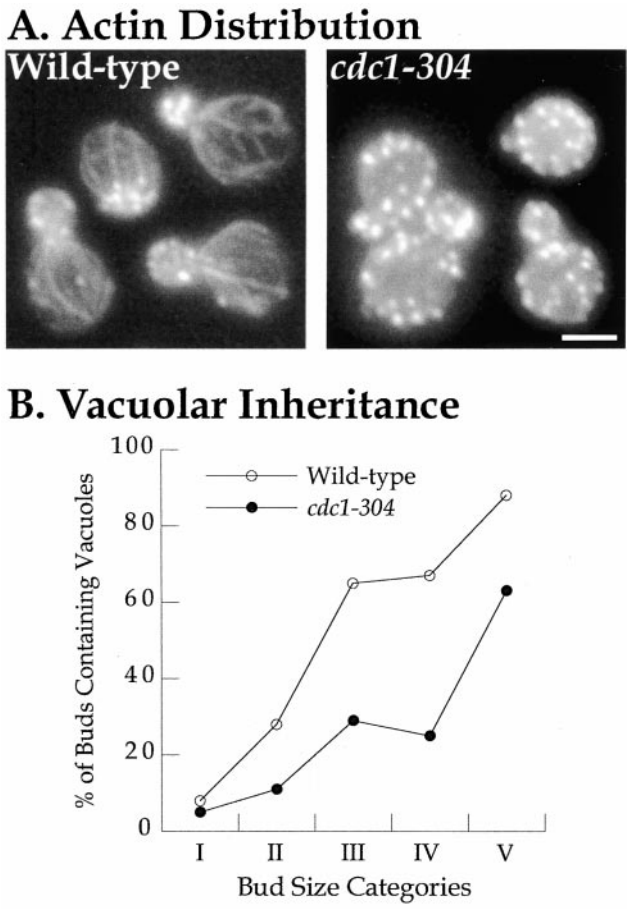

Figure 4. The *cdc1-304* mutant exhibits defects in actin polarity and vacuolar inheritance. (A) Wild-type (BGY316) and *cdc1-304* (BGY111) cultures were grown at room temperature, shifted to 37°C for 1 h, fixed, and stained with Alexa 594–phalloidin. Fluorescence images are shown. Most of the wild-type cells contain polarized actin patches and cables, whereas most of the *cdc1-304* cells contain depolarized patches and few visible cables. (B) Wild-type and *cdc1-304* cultures were grown at room temperature, labeled with FM4-64, and then shifted to 37°C for 1 h. The presence of maternally derived vacuolar material in the bud was quantified as described in the legend to Fig. 2 C. The *cdc1-304* mutant shows a delay in vacuolar inheritance. Bar, 2 μm.

and undivided nuclei (Hartwell et al., 1970). However, subsequent work indicated that *cdc1* cells can arrest either without a bud or with a small bud, pointing to a role for Cdc1p at multiple stages of the cell cycle (Hartwell, 1971; Paidhungat and Garrett, 1998b). This heterogeneous arrest phenotype discounts *CDC1* as a true cell division cycle gene. Recent studies suggest a link between Cdc1p and divalent cation metabolism (see Discussion), but the function and localization of Cdc1p are unknown. Therefore, we undertook further experiments to clarify the role of Cdc1p in Golgi inheritance.

The cdc1-304 Mutant Shows Defects in Actin Organization and Golgi Retention

The first question was whether the polarity defects in *cdc1* cells are restricted to Golgi inheritance. We examined actin distribution in wild-type and *cdc1-304* cultures that had been incubated at 37°C for 1 h (Fig. 4 A). In wild-type cells, actin patches are concentrated at sites of polarized growth, and cables are visible in the mother cells. By contrast, actin polarity is largely abolished in *cdc1-304* cells; patches are distributed evenly throughout the mother and bud, and cables are rarely visible. Because a polarized actin cytoskeleton is needed for vacuolar inheritance (Catlett and Weisman, 2000), this process should also be disrupted by the *cdc1-304* mutation. Indeed, vacuolar inheritance at 37°C is slower in the *cdc1-304* strain than in the corresponding wild-type strain (Fig. 4 B). Vacuolar morphology is also abnormal in the *cdc1-304* strain, with many of the cells containing clusters of vacuolar fragments (not shown). These data indicate that Cdc1p influences the distribution of multiple cellular components.

Can the defective inheritance of Sec7p–GFP in *cdc1-304* cells be explained by the loss of actin polarity? We found previously that when the actin cytoskeleton is extensively disrupted with LatA, Sec7p–GFP is still inherited efficiently (Fig. 2). However, because LatA selectively inhibits actin polymerization (Ayscough et al., 1997), any polymerized actin structures will not be affected by this drug. We speculate that the bud contains residual actin structures that are resistant to disruption by LatA (Karpova et al., 2000) and that a subset of the late Golgi elements are retained in the bud by association with this residual bud-localized actin. Presumably, the *cdc1-304* mutation inhibits late Golgi inheritance by disrupting not only the actin cables but also the bud-localized actin. This model predicts that in a *cdc1-304* cell, Sec7p–GFP should localize to the bud but will fail to be retained there. To test this prediction, we repeatedly imaged Sec7p–GFP in individual *CDC1* and *cdc1-304* cells at 37°C (Fig. 5). Complete confocal *z*-stacks were captured at intervals of 2.5 s. Because the Golgi of *S. cerevisiae* is highly dynamic (Wooding and Pelham, 1998), the overall pattern of Sec7p–GFP fluorescence changes significantly between each time point, even with this rapid imaging protocol; but we were able to assess the gain or loss of fluorescence in small buds. As expected, the bud of a typical *CDC1* cell almost always contains Sec7p–GFP (not shown). By contrast, the bud of a typical *cdc1-304* mutant cell alternately contains and lacks Sec7p–GFP (Fig. 5). This result confirms that the buds of *cdc1-304* cells are viable and fits with our hypothesis that Cdc1p function is needed to retain late Golgi elements in the bud.

Sec7p–GFP Inheritance Is Inhibited by the myo2-66 Mutation

We conjectured that both the actin-dependent transport and the retention of Golgi elements might involve Myo2p, an essential type V myosin (Johnston et al., 1991). Myo2p has been implicated in the transport of organelles toward sites of polarized growth (Pruyne and Bretscher, 2000). Moreover, Myo2p shows a weak concentration in the bud even in LatA-treated cells (Ayscough et al., 1997).

To test whether Myo2p functions in Golgi inheritance, we took advantage of the well-characterized *myo2-66* allele, which encodes a protein with a point mutation in the actin-binding motor domain (Lillie and Brown, 1994). At 23°C, actin organization in *myo2-66* cells is essentially normal (Johnston et al., 1991; Rossanese, O.W., unpublished

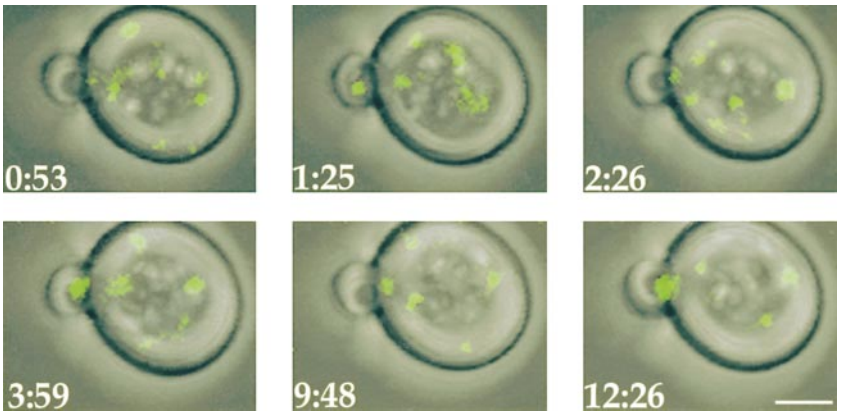

Figure 5. The small buds of *cdc1-304* cells repeatedly lose and regain late Golgi elements. Shown are merged fluorescence and transmitted light projections of a representative budded *cdc1-304* cell, which had been incubated at 37°C for 2 h when imaging was initiated. These selected frames from the time series demonstrate that the bud alternately contains and lacks detectable Sec7p–GFP fluorescence. Bar, 2 μm.

observations), but vacuolar inheritance is severely compromised (Hill et al., 1996). We introduced the *myo2-66* allele into our standard yeast strain and examined cells grown at 23°C. Like *cdc1-304* cells, *myo2-66* cells exhibit pronounced defects in the inheritance of vacuoles and Sec7p–GFP (Fig. 6, A and B). These findings suggest that Myo2p participates in the transport and retention of late Golgi elements.

Cdc1p and Myo2p Are Required for Normal Inheritance of the Late Golgi Marker Ric1p–GFP

All of the experiments described so far used Sec7p–GFP as the late Golgi marker. Thus, we were concerned that our data might reflect the specific behavior of Sec7p–GFP rather than the general behavior of late Golgi elements. To exclude this possibility, we sought to create a second GFP-labeled marker for the late Golgi apparatus. This task was not straightforward because many late Golgi proteins also localize to endosomes; indeed, Sec7p is one of the few proteins that is thought to be specific for the late Golgi apparatus (Lewis et al., 2000). However, Siniossoglou and colleagues (2000) recently reported that Ric1p forms part of a protein complex that partially colocalizes with Sec7p at the late Golgi apparatus. Ric1p–GFP yields a punctate fluorescence pattern in living cells (Fig. 7 A). In *cdc1-304* and *myo2-66* cells, Ric1p–GFP inheritance is significantly reduced during the earliest stages of bud growth (Fig. 7 B), although the inheritance defects are somewhat less severe than those observed with Sec7p–GFP (see above). This result confirms that Cdc1p and Myo2p play a general role in the inheritance of late Golgi elements.

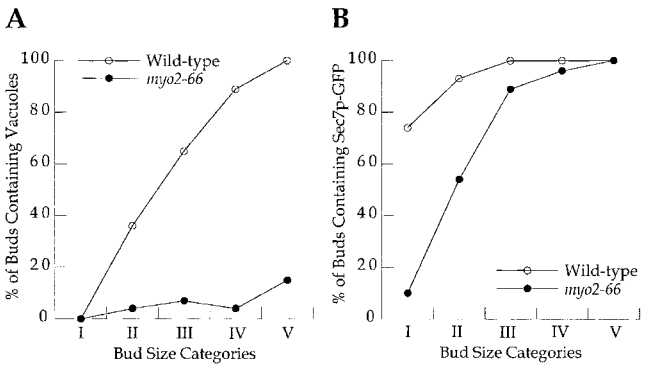

Figure 6. Defective inheritance of vacuoles and Sec7p–GFP in *myo2-66* cells. Cultures carrying the wild-type *MYO2* gene (strain BGY316; ○) or the *myo2-66* allele (strain BGY415; ●) were grown at 23°C and assayed as in Fig. 2 for the inheritance of vacuoles (A) or Sec7p–GFP (B).

Early and Late Golgi Elements Are Inherited by Distinct Pathways

How are early Golgi elements inherited in *S. cerevisiae*? Here we are defining the early Golgi as the cis- and medial-Golgi cisternae that do not label with Sec7p–GFP. To monitor the inheritance of early Golgi elements, we created two additional GFP-labeled marker proteins. For the first marker, GFP was linked to the COOH terminus of Sec21p, which is the γ-COP subunit of the COPI coatomer (Hosobuchi et al., 1992). Vertebrate COPI is present at all levels of the Golgi stack except possibly the trans-most cisternae (Oprins et al., 1993; Orci et al., 1997; Ladinsky et

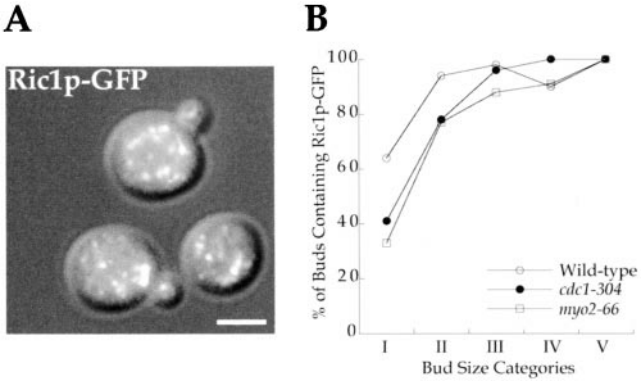

Figure 7. Creation of a second late Golgi marker. (A) Representative cells expressing *RIC1–GFPx3*. Shown is a merged DIC and fluorescence image. (B) Inheritance of Ric1p–GFP in wild-type and mutant cells. As described in the legend to Fig. 3 B, a wild-type strain (○), a *cdc1-304* strain (●), and a *myo2-66* strain (□) were assayed for the inheritance of Ric1p–GFP. The wild-type and *cdc1-304* strains were grown at 23°C and then shifted to 37°C for 1 h before fixation. The *myo2-66* strain was maintained at 23°C before fixation, but the *myo2-66* data can be compared with the wild-type data because Golgi inheritance in wild-type cells is unaffected by shifting to 37°C for 1 h (not shown). The inheritance of Ric1p–GFP is significantly inhibited by the *cdc1-304* and *myo2-66* mutations. Bar, 2 μm.

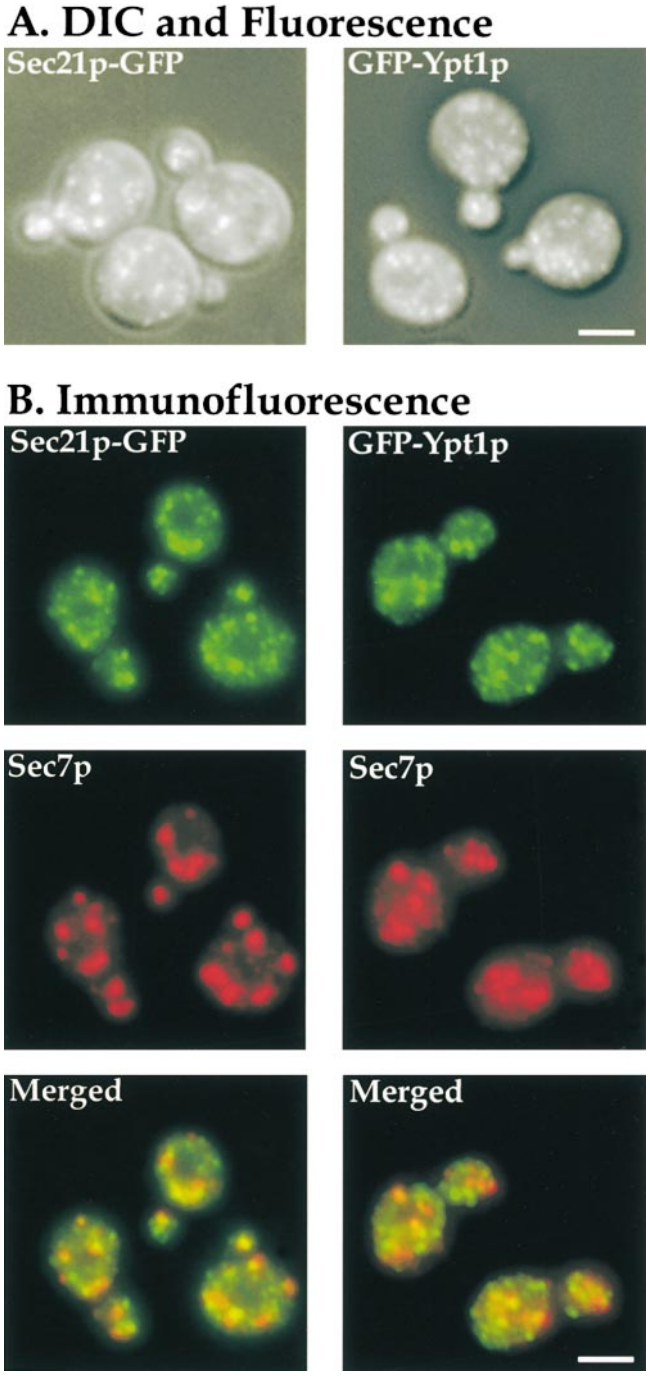

Figure 8. Creation of two additional GFP-labeled Golgi markers. (A) Representative cells expressing *SEC21-GFPx3* or *GFP-YPT1*. Shown are merged DIC and fluorescence images. (B) Double label immunofluorescence of Sec7p with either Sec21p–GFP or GFP–Ypt1p. Fixed cells were labeled with polyclonal anti-Sec7p antibody followed by Rhodamine red-X–conjugated anti–rabbit antibody (red) and with monoclonal anti-GFP antibody followed by Cy2-conjugated anti–mouse antibody (green). As shown in the merged images, Sec7p shows partial colocalization with Sec21p–GFP but no significant colocalization with GFP–Ypt1p. Bars, 2 μm.

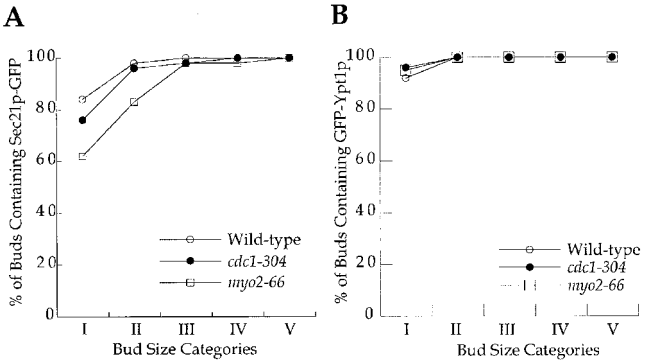

Figure 9. Inheritance of early Golgi markers in wild-type and mutant cells. As described in the legend to Fig. 3 B, wild-type strains (○), *cdc1-304* strains (●), and *myo2-66* strains (□) were assayed for the inheritance of Sec21p–GFP (A) and GFP–Ypt1p (B). The wild-type and *cdc1-304* strains were grown at 23°C and then shifted to 37°C for 1 h before fixation, whereas the *myo2-66* strains were maintained at 23°C before fixation (see Fig. 7). The inheritance of Sec21p–GFP is unaffected by the *cdc1-304* mutation and is inhibited only slightly by the *myo2-66* mutation, whereas the inheritance of GFP–Ypt1p is not affected by either mutation.

al., 1999). Several of the vertebrate COPI subunits are found on both Golgi membranes and endosomes, but γ-COP is restricted to the Golgi complex (Whitney et al., 1995; Gu and Gruenberg, 1999), suggesting that Sec21p should be a specific marker for the Golgi in yeast. Sec21p–GFP labels multiple punctate structures per cell (Fig. 8 A) and exhibits partial colocalization (not shown) with the medial-Golgi marker Mnt1p/Kre2p (Jungmann and Munro, 1998; Lussier et al., 1995). In addition, Sec21p–GFP exhibits partial colocalization with Sec7p (Fig. 8 B). Thus, Sec21p–GFP marks both early and late Golgi elements. For the second additional Golgi marker, GFP was fused to the NH_2 terminus of Ypt1p, a small GTPase that regulates membrane traffic at early stages of intra-Golgi transport (Segev et al., 1988; Preuss et al., 1992; Jedd et al., 1995). GFP–Ypt1p labels multiple punctate structures per cell (Fig. 8 A). As expected, GFP–Ypt1p exhibits no significant colocalization with Sec7p (Fig. 8 B), confirming that GFP–Ypt1p exclusively marks the early Golgi.

Like late Golgi markers, Sec21p–GFP and GFP–Ypt1p are present in most of the small buds during normal growth (Fig. 8 A) or after LatA treatment (not shown). However, as judged by the plus–minus visual assay, Sec21p–GFP and GFP–Ypt1p are inherited normally in strains carrying the *cdc1-304* allele (Fig. 9). In the case of Sec21p–GFP, the *cdc1-304* mutation presumably blocks the inheritance of Sec21p–GFP-containing late Golgi elements but not of Sec21p–GFP-containing early Golgi elements. The *myo2-66* mutation has only a mild inhibitory effect on Sec21p–GFP inheritance and has no effect on GFP–Ypt1p inheritance (Fig. 9). These data suggest that early Golgi elements can localize to the bud independently of Cdc1p and Myo2p. We conclude that in *S. cerevisiae*, early Golgi elements and late Golgi elements are inherited by distinct pathways.

One possible mechanism for early Golgi inheritance would be the de novo formation of Golgi cisternae from ER membranes. Previous electron microscopy data indicated that peripheral ER membranes are present in the bud early in the cell cycle (Preuss et al., 1991). We have verified this observation using fluorescence microscopy. To visualize the ER, the Kar2p presequence was linked to GFP, and a COOH-terminal HDEL tetrapeptide was added to retain the protein in the ER lumen (Pelham, 1995; Zheng and

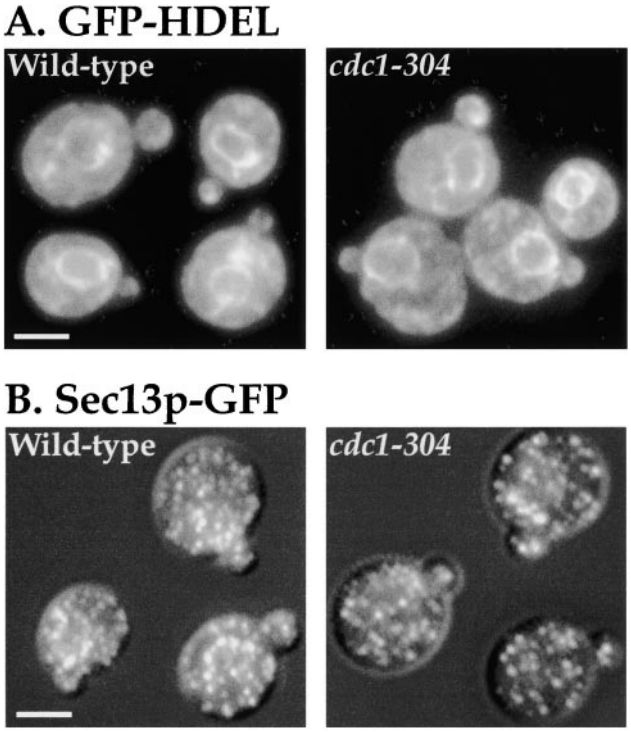

Figure 10. The ER and tER are inherited normally in *cdc1-304* cells. (A) Fluorescence images of wild-type (BGY418) and *cdc1-304* (BGY419) strains expressing *GFP–HDEL*. This protein marks the nuclear envelope as well as peripheral ER membranes. Cells were grown at 23°C and then shifted to 37°C for 1 h before fixation. (B) Merged DIC and fluorescence images of wild-type (BGY318) and *cdc1-304* (BGY110) strains expressing *SEC13-GFP*. This fusion protein marks the nascent COPII vesicles that define the tER. Both the ER and the tER localize to small buds with undiminished efficiency in the *cdc1-304* mutant. Bars, 2 μm.

Gierasch, 1996). GFP–HDEL highlights the nuclear envelope as well as peripheral ER elements (Fig. 10 A). We find that >95% of the small buds contain GFP–HDEL from the earliest stages of bud development. To confirm that bud-localized ER membranes are capable of functioning as tER, we generated cells in which the COPII coat protein Sec13p (Pryer et al., 1993) was tagged with GFP. Sec13p-GFP labels multiple fluorescent specks (Fig. 10 B) that presumably represent COPII vesicles budding throughout the ER network (Rossanese et al., 1999). Like GFP–HDEL, Sec13p-GFP is visible in virtually all of the buds. Hence, it is plausible that the ER membranes present in the bud could generate early Golgi elements. As predicted by this model, ER and tER inheritance are unaffected by the *cdc1-304* mutation (Fig. 10) or the *myo2-66* mutation (not shown). This observation may explain why early Golgi elements are inherited efficiently in *cdc1-304* cells and *myo2-66* cells.

Discussion

In budding yeasts, organellar inheritance is not directly coupled to cell division. This feature has made *S. cerevisiae* a productive system for studying mitochondrial and vacuolar inheritance (Yaffe, 1999; Catlett and Weisman, 2000). A portion of the mitochondrial and vacuolar material present in the mother cell is transferred into the bud. However, when vacuolar transfer is inhibited, the daughter cells still acquire a vacuole, probably via the fusion of Golgi-derived vesicles with endocytic vesicles (Hill et al., 1996; Gomes De Mesquita et al., 1997). This type of de novo formation of compartments may be a general feature of the exocytic and endocytic pathways (Glick and Malhotra, 1998). Thus, the inheritance of various yeast organelles involves either transfer from the mother cell into the bud, de novo formation in the bud, or both.

Inheritance of Late Golgi Elements

Golgi inheritance has not previously been analyzed at the molecular genetic level in yeast. The inheritance of the vertebrate Golgi has been studied (Lowe et al., 1998; Thyberg and Moskalewski, 1998), but the vertebrate Golgi differs from the *S. cerevisiae* Golgi in several ways. First, the vertebrate Golgi is organized into stacks. Second, the vertebrate Golgi breaks down during mitosis, whereas the *S. cerevisiae* Golgi remains intact throughout the cell cycle (Preuss et al., 1992; Lowe et al., 1998). Third, vertebrate Golgi dynamics are strongly influenced by microtubules, whereas in *S. cerevisiae*, microtubules have not been implicated in the dynamics of any organelle except the nucleus (Botstein et al., 1997). Consistent with this latter observation, we find that depolymerization of microtubules in *S. cerevisiae* has no detectable effect on the distribution or inheritance of Golgi elements (Fig. 1 C; data not shown).

How might Golgi cisternae in *S. cerevisiae* localize to the bud? One obvious possibility is actin-dependent transport from the mother cell into the bud (Preuss et al., 1992). Actin is known to direct the transport of secretory vesicles and other structures to sites of polarized growth (Botstein et al., 1997). However, another possibility is that Golgi cisternae grow out of peripheral ER membranes, which are present in the bud from an early stage in bud development (Preuss et al., 1991). We set out to test whether one or both of these mechanisms contributes to Golgi inheritance in *S. cerevisiae*. Most of our experiments used a Sec7p–GFP fusion protein as the Golgi marker (Séron et al., 1998). Sec7p is an abundant component of late Golgi cisternae (Franzusoff et al., 1991; Lewis et al., 2000), and the Sec7p–GFP fusion gives a robust fluorescence signal.

Sec7p–GFP fluorescence is often concentrated at sites of polarized growth, but only in cells that contain an intact actin cytoskeleton (Fig. 1). A simple model to explain these observations is that late Golgi elements are transported along actin cables by a myosin motor. Yet, surprisingly, when actin is depolymerized with LatA, some Sec7p–GFP is still present in the small buds (Fig. 2). In other words, disrupting the actin cytoskeleton reduces but does not abolish the inheritance of late Golgi elements. These data suggest that late Golgi elements are transported into the bud along actin cables but that a subset of the late Golgi elements can localize to the bud, even when actin cables have been eliminated using LatA (Fig. 11 B). The LatA-resistant inheritance mechanism might be independent of actin, or it might involve residual actin structures that are resistant to depolymerization by LatA (Karpova et al., 2000).

cdc1 Mutants Are Defective in the Inheritance of Late Golgi Elements

To identify proteins involved in Golgi inheritance, we used a visual screen to isolate 14 temperature-sensitive mutants with defects in localizing Sec7p–GFP to the bud (Fig. 3).

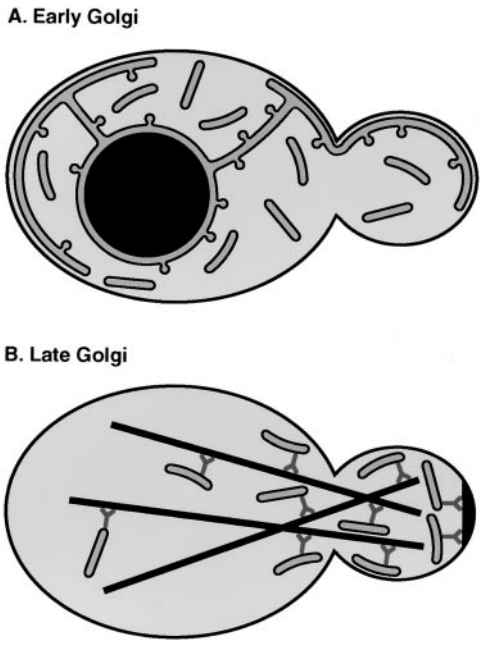

Figure 11. Model for Golgi inheritance in *S. cerevisiae*. (A) Inheritance of early Golgi elements. The ER comprises the nuclear envelope plus peripheral ER membranes. COPII vesicles bud throughout the ER network, thereby generating early Golgi cisternae in both the mother cell and the bud. The inheritance of early Golgi elements requires ER inheritance but does not directly require actin cables, Myo2p or Cdc1p. (B) Inheritance of late Golgi elements. Dimeric Myo2p molecules bind to late Golgi cisternae and transport these cisternae along actin cables into the bud. Additional Myo2p molecules retain a subset of the late Golgi cisternae in the bud by binding to actin or other bud components. Cdc1p is required to maintain a polarized actin cytoskeleton and to retain late Golgi cisternae in the bud.

Complementation analysis revealed that all 14 mutants carry alleles of *CDC1*. Therefore, we concentrated on characterizing a representative mutant, which was designated *cdc1-304*. This mutant is also defective in the inheritance of the late Golgi protein Ric1p–GFP (Fig. 7 B), confirming that *cdc1* mutants have a general block in the inheritance of late Golgi elements. Despite the gene name, *cdc1* mutants are not defective in cell division control; instead, they show growth inhibition during bud formation and bud expansion (Hartwell, 1971; Paidhungat and Garrett, 1998b). Genetic studies indicate that Cdc1p function is linked to divalent cation metabolism, although the nature of this link is still uncertain (Loukin and Kung, 1995; Paidhungat and Garrett, 1998a,b). The only characterized homologue of *CDC1* is the *Neurospora crassa frost* gene, which has been implicated in polarized growth and divalent cation metabolism (Sone and Griffiths, 1999). It seems likely that Cdc1p and divalent cations are both needed for some aspect of polarized growth. Therefore, the effect of *cdc1* mutations on Golgi inheritance seems to reflect a more global role of Cdc1p.

In addition to showing growth inhibition at multiple stages of the cell cycle, *cdc1* mutants are defective in schmoo formation (Paidhungat and Garrett, 1998b; Rossanese, O.W., unpublished observations). A possible explanation for these diverse phenotypes comes from our finding that *cdc1* mutants have a depolarized actin cytoskeleton (Fig. 4 A). *cdc1* mutants also exhibit reduced vacuolar inheritance (Fig. 4 B), probably because of their depolarized actin. Understanding the effects of *cdc1* mutations will require elucidating the specific function of Cdc1p. The predicted sequence of this protein (Halbrook and Hoekstra, 1994) yields little information, except that Cdc1p is likely to be an integral membrane protein. Our current efforts are directed at determining the localization and topology of Cdc1p.

Presumably, *cdc1* mutants were identified in our screen because they are defective not only in the actin-dependent transport of late Golgi elements but also in the LatA-resistant localization of late Golgi elements to the bud. This reasoning explains why the screen yielded only a single gene: *CDC1* is apparently one of the few genes that is needed for both aspects of late Golgi inheritance. What is the LatA-resistant mechanism that localizes a subset of the late Golgi elements to the bud? Our data suggest that a subset of the late Golgi elements are retained in the bud (Figs. 5 and 11 B). Cdc1p is evidently required for this retention, either as a component of the retention system or as a regulatory factor that allows retention to occur. An attractive possibility is that retention involves bud-localized actin structures that are stable in the presence of LatA but labile in the absence of Cdc1p function.

The myo2-66 Mutation Blocks the Inheritance of Late Golgi Elements

We surmised that the two inheritance mechanisms for the late Golgi, actin-dependent transport and LatA-resistant retention, might both involve Myo2p, a dimeric type V myosin (Brown, 1997; Beningo et al., 2000). Actin-dependent transport of organelles is usually performed by type V myosins (Wu et al., 2000). Myo2p is the only essential myosin in *S. cerevisiae*, and it has previously been implicated in the transport of secretory vesicles, vacuoles, and chitosomes to sites of polarized growth (Govindan et al., 1995; Hill et al., 1996; Santos and Snyder, 1997; Schott et al., 1999). (*S. cerevisiae* also contains a second type V myosin called Myo4p, but this protein seems to be specialized for mRNA transport [Long et al., 1997; Takizawa et al., 1997; Schott et al., 1999].) Intriguingly, a fraction of the Myo2p molecules may be retained in the bud even after LatA treatment (Ayscough et al., 1997). To test whether Myo2p plays a role in the inheritance of late Golgi elements, we generated strains that carry the *myo2-66* allele (Johnston et al., 1991; Lillie and Brown, 1994). We find that *myo2-66* cells are defective in the inheritance of Sec7p–GFP (Fig. 6 B) and Ric1p–GFP (Fig. 7 B). A likely explanation is that the *myo2-66* allele inhibits the Myo2p-driven transport of late Golgi elements to sites of polarized growth. In addition, the *myo2-66* allele evidently reduces the retention of late Golgi elements in the bud. The *myo2-66* allele encodes a point mutation in the NH_2-terminal actin-binding domain of Myo2p (Lillie and Brown, 1994), whereas previous studies have hinted that the COOH-terminal tail domain might be responsible for tethering Myo2p in the bud (Catlett and Weisman, 1998; Reck-Peterson et al., 1999). However, the evidence for tail-dependent tethering is still ambiguous (Schott et al., 1999; Karpova et al., 2000), and it is equally possible that the NH_2-terminal domain of Myo2p binds to bud-localized actin, thereby retaining late Golgi elements

in the bud (Mehta et al., 1999). This hypothesis fits with the idea that the bud contains actin structures that are resistant to depolymerization by LatA. Regardless of the precise mechanism, our data suggest that Myo2p is required for both the transport and the retention of late Golgi elements.

We propose the following model for inheritance of the late Golgi (Fig. 11 B). Myo2p attaches to late Golgi elements and transports them to sites of polarized growth, including small buds. This Myo2p-dependent transport is efficient only in rapidly growing cells. However, Golgi inheritance is efficient under all growth conditions because a subset of the late Golgi elements are retained in the bud via the interaction of Myo2p with bud-localized actin or with other partner proteins. The *myo2-66* mutation blocks late Golgi inheritance by inhibiting both the transport and the retention of late Golgi elements. Similarly, *cdc1* mutations inhibit the transport of late Golgi elements by disrupting actin cables, and they inhibit the retention of late Golgi elements by disrupting bud-localized actin or other components that are needed to immobilize Myo2p in the bud.

Testing these ideas will require characterizing the proteins that mediate the interactions between Golgi elements, Myo2p, and bud components. How can we identify these proteins? Insights may come from the mutants with abnormal Golgi morphology that were isolated in our screen (Fig. 3 A). The class B mutant cells contain a small number of enlarged Golgi elements. A similar Golgi pattern is seen in yeast strains with reduced activity of the Arf GTPase (Gaynor et al., 1998a), suggesting that the primary defect in the class B mutants probably lies in Golgi function rather than Golgi distribution. More promising are the class C mutants, in which late Golgi elements show enhanced localization to sites of polarized growth. In addition, the single class D mutant exhibits strikingly abnormal Golgi morphology and also has an altered actin cytoskeleton (Rossanese, O.W., unpublished observations). A genetic analysis of the class C and D mutants should illuminate the interactions between Golgi elements and the actin cytoskeleton.

Early and Late Golgi Elements Are Inherited by Distinct Pathways

To explore the inheritance of early Golgi elements, we made GFP fusions to Sec21p, a component of the COPI coat complex (Duden et al., 1994; Gaynor et al., 1998b), and Ypt1p, a small GTPase that regulates membrane traffic at the early Golgi (Segev et al., 1988; Jedd et al., 1995). Sec21p–GFP localizes to both early and late Golgi elements, whereas GFP–Ypt1p localizes specifically to early Golgi elements (Fig. 8). Interestingly, the inheritance of Sec21p–GFP and GFP–Ypt1p is largely unaffected by either the *cdc1-304* mutation or the *myo2-66* mutation (Fig. 9). These data do not exclude the possibility that early Golgi elements undergo the same type of transport and retention as late Golgi elements; indeed, early Golgi markers are sometimes concentrated at sites of polarized growth (Segev et al., 1988; Preuss et al., 1992; Rossanese, O.W., unpublished observations). However, early Golgi elements still localize efficiently to the bud after inhibition of Cdc1p or Myo2p function, implying that early Golgi elements are inherited by a pathway distinct from that used by late Golgi elements.

We favor the idea that early Golgi cisternae are generated de novo in the bud from ER membranes (Fig. 11 A). Consistent with this model, ER and tER markers are inherited very early, even in *cdc1-304* and *myo2-66* cells (Fig. 10). The early Golgi cisternae that are generated in the bud presumably mature into late Golgi cisternae (Wooding and Pelham, 1998; Morin-Ganet et al., 2000). If so, then why are late Golgi elements absent from the small buds of *cdc1-304* and *myo2-66* cells? Presumably, Golgi retention is inhibited by the *cdc1-304* and *myo2-66* mutations, so maturing cisternae can diffuse out of a small bud into the mother cell, yielding a bud that contains early but not late Golgi elements. When the bud becomes larger, most of the maturing cisternae that were generated in the bud will remain there, and indeed, buds larger than 7.5% of the average mother cell volume almost always contain late Golgi elements, even in *cdc1-304* and *myo2-66* strains (Figs. 3 B and 6 B). These ideas will remain speculative until we find conditions that block the transfer of ER membranes into the bud.

Why does *S. cerevisiae* ensure that the nascent bud contains both early and late Golgi elements? One likely reason is that when late Golgi elements are located at sites of polarized growth, secretory vesicles can reach their destinations more rapidly (Preuss et al., 1992). Even if the cells are growing slowly, bud development may be more efficient if the bud contains a complete set of secretory organelles.

Relevance to Golgi Inheritance in Other Eukaryotes

Some aspects of Golgi inheritance in *S. cerevisiae* probably reflect the specific characteristics of this organism. Most other eukaryotes contain organized Golgi stacks, so early and late Golgi elements in those cells are presumably inherited as a unit. For example, the budding yeast *Pichia pastoris* is closely related to *S. cerevisiae*, yet *P. pastoris* has stacked Golgi organelles next to discrete tER sites (Gould et al., 1992; Rossanese et al., 1999). It will be interesting to perform a comparative analysis of Golgi inheritance in *P. pastoris* and *S. cerevisiae*.

Despite the differences in Golgi organization between *S. cerevisiae* and vertebrate cells, the basic mechanisms of Golgi inheritance seem to be similar. Early in vertebrate mitosis, the Golgi ribbon breaks down into fragments that more closely resemble the yeast Golgi (Lowe et al., 1998; Thyberg and Moskalewski, 1998). These vertebrate Golgi fragments then appear to partition between the daughter cells, just as late Golgi elements in *S. cerevisiae* partition between the mother cell and the bud. Late in vertebrate mitosis, Golgi components may emerge from the ER to generate new Golgi stacks (Zaal et al., 1999); by analogy, we propose that early Golgi cisternae in *S. cerevisiae* arise de novo from ER membranes that are present in the bud. Ongoing studies of these two experimental systems should reveal evolutionarily conserved principles of Golgi inheritance.

Thanks for strains and reagents to Natalie Catlett, Lois Weisman, Peter Rubenstein, Nava Segev, David Drubin, Daniel Schott, Anthony Bretscher, Alex Franzusoff, and Mark Hochstrasser. We are especially grateful to Judith Austin and her colleagues for use of their fluorescence microscope, and to Craig Lassy and Tim Karr for help with confocal mi-

croscopy. Thanks to Stephen Garrett, Nava Segev, Bob McCarroll, and the members of the Glick laboratory for helpful discussions, and to Olivia Casanueva for generating the *GFP–YPT1* construct.

O.W. Rossanese, C. Reinke, B.J. Bevis, and A.T. Hammond were supported in part by National Institutes of Health training grant 5-20942. This work was funded by National Science Foundation grant MCB-9604342, National Institutes of Health grant GM61156, and an award from the Pew Charitable Trusts.

Submitted: 14 August 2000
Revised: 19 December 2000
Accepted: 29 January 2001

References

Antebi, A., and G.R. Fink. 1992. The yeast Ca^{2+}-ATPase homologue, PMR1, is required for normal Golgi function and localizes in a novel Golgi-like distribution. *Mol. Biol. Cell*. 3:633–654.

Ayscough, K.R., and D.G. Drubin. 1996. ACTIN: general principles from studies in yeast. *Annu. Rev. Cell Dev. Biol.* 12:129–160.

Ayscough, K.R., J. Stryker, N. Pokala, M. Sanders, P. Crews, and D.G. Drubin. 1997. High rates of actin filament turnover in budding yeast and roles for actin in establishment and maintenance of cell polarity revealed using the actin inhibitor latrunculin-A. *J. Cell Biol.* 137:399–416.

Baba, M., N. Baba, Y. Ohsumi, K. Kanaya, and M. Osumi. 1989. Three-dimensional analysis of morphogenesis induced by mating pheromone α factor in *Saccharomyces cerevisiae*. *J. Cell Sci.* 94:207–216.

Bannykh, S.I., and W.E. Balch. 1997. Membrane dynamics at the endoplasmic reticulum–Golgi interface. *J. Cell Biol.* 138:1–4.

Beningo, K.A., S.H. Lillie, and S.S. Brown. 2000. The yeast kinesin-related protein Smy1p exerts its effects on the class V myosin Myo2p via a physical interaction. *Mol. Biol. Cell*. 11:691–702.

Botstein, D., D. Amberg, J. Mulholland, T. Huffaker, A. Adams, D. Drubin, and T. Stearns. 1997. The yeast cytoskeleton. *In* The Molecular and Cellular Biology of the Yeast *Saccharomyces*. Vol. 3. J.R. Pringle, J.R. Broach, and E.W. Jones, editors. Cold Spring Harbor Laboratory Press, Cold Spring Harbor, NY. 1–90.

Brown, S.S. 1997. Myosins in yeast. *Curr. Opin. Cell Biol.* 9:44–48.

Catlett, N.L., and L.S. Weisman. 1998. The terminal tail region of a yeast myosin-V mediates its attachment to vacuole membranes and sites of polarized growth. *Proc. Natl. Acad. Sci. USA*. 95:14799–14804.

Catlett, N.L., and L.S. Weisman. 2000. Divide and multiply: organelle partitioning in yeast. *Curr. Opin. Cell Biol.* 12:509–516.

Cook, R.K., W.T. Blake, and P.A. Rubenstein. 1992. Removal of the amino-terminal acidic residues of yeast actin. Studies in vitro and in vivo. *J. Biol. Chem.* 267:9430–9436.

Drubin, D.G., H.D. Jones, and K.F. Wertman. 1993. Actin structure and function: roles in mitochondrial organization and morphogenesis in budding yeast and identification of the phalloidin-binding site. *Mol. Biol. Cell*. 4:1277–1294.

Duden, R., M. Hosobuchi, S. Hamamoto, M. Winey, B. Byers, and R. Schekman. 1994. Yeast beta- and beta′-coat proteins (COP). Two coatomer subunits essential for endoplasmic reticulum-to-Golgi traffic. *J. Biol. Chem.* 269: 24486–24495.

Franzusoff, A., K. Redding, J. Crosby, R.S. Fuller, and R. Schekman. 1991. Localization of components involved in protein transport and processing through the yeast Golgi apparatus. *J. Cell Biol.* 112:27–37.

Gaynor, E.C., C.Y. Chen, S.D. Emr, and T.R. Graham. 1998a. ARF is required for maintenance of yeast Golgi and endosome structure and function. *Mol. Biol. Cell*. 9:653–670.

Gaynor, E.C., T.R. Graham, and S.D. Emr. 1998b. COPI in ER/Golgi and intra-Golgi transport: do yeast COPI mutants point the way? *Biochim. Biophys. Acta*. 1404:33–51.

Gietz, R.D., and A. Sugino. 1988. New yeast-*Escherichia coli* shuttle vectors constructed with in vitro mutagenized yeast genes lacking six-base pair restriction sites. *Gene*. 74:527–534.

Glick, B.S., and V. Malhotra. 1998. The curious status of the Golgi apparatus. *Cell*. 95:883–889.

Gomes De Mesquita, D.S., J. Shaw, J.A. Grimbergen, M.A. Buys, L. Dewi, and C.L. Woldringh. 1997. Vacuole segregation in the *Saccharomyces cerevisiae vac2-1* mutant: structural and biochemical quantification of the segregation defect and formation of new vacuoles. *Yeast*. 13:999–1008.

Gould, S.J., D. McCollum, A.P. Spong, J.A. Heyman, and S. Subramani. 1992. Development of the yeast *Pichia pastoris* as a model organism for a genetic and molecular analysis of peroxisome assembly. *Yeast*. 8:613–628.

Govindan, B., R. Bowser, and P. Novick. 1995. The role of Myo2, a yeast class V myosin, in vesicular transport. *J. Cell Biol.* 128:1055–1068.

Gu, F., and J. Gruenberg. 1999. Biogenesis of transport intermediates in the endocytic pathway. *FEBS Lett.* 452:61–66.

Halbrook, J., and M.F. Hoekstra. 1994. Mutations in the *Sacharomyces cerevisiae CDC1* gene affect double-strand-break-induced intrachromosomal recombination. *Mol. Cell. Biol.* 14:8037–8050.

Hammond, A.T., and B.S. Glick. 2000a. Dynamics of transitional endoplasmic reticulum sites in vertebrate cells. *Mol. Biol. Cell*. 11:3013–3030.

Hammond, A.T., and B.S. Glick. 2000b. Raising the speed limits for 4D fluorescence microscopy. *Traffic*. 1:935–940.

Harlow, E., and D. Lane. 1988. Antibodies. A Laboratory Manual. Cold Spring Harbor Laboratory Press, Cold Spring Harbor, NY. 726 pp.

Hartwell, L. 1971. Genetic control of the cell division cycle IV. Genes controlling bud emergence and cytokinesis. *Exp. Cell Res.* 69:265–276.

Hartwell, L.H., J. Culotti, and B. Reid. 1970. Genetic control of the cell-division cycle in yeasts. I. Detection of mutants. *Proc. Natl. Acad. Sci. USA*. 66:352–359.

Hildebrandt, E.R., and M.A. Hoyt. 2000. Mitotic motors in *Saccharomyces cerevisiae*. *Biochim. Biophys. Acta*. 1496:99–116.

Hill, K.L., N.L. Catlett, and L.S. Weisman. 1996. Actin and myosin function in directed vacuole movement during cell division in *Saccharomyces cerevisiae*. *J. Cell Biol.* 135:1535–1549.

Ho, S.N., H.D. Hunt, R.M. Horton, J.K. Pullen, and L.R. Pease. 1989. Site-directed mutagenesis by overlap extension using the polymerase chain reaction. *Gene*. 77:51–59.

Hosobuchi, M., T. Kreis, and R. Schekman. 1992. SEC21 is a gene required for ER to Golgi protein transport that encodes a subunit of a yeast coatomer. *Nature*. 360:603–605.

Jacobs, C.W., A.E.M. Adams, P.J. Szaniszlo, and J.R. Pringle. 1988. Functions of microtubules in the *Saccharomyces cerevisiae* cell cycle. *J. Cell Biol.* 107: 1409–1426.

Jedd, G., C.J. Richardson, R.J. Litt, and N. Segev. 1995. The Ypt1 GTPase is essential for the first two steps of the yeast secretory pathway. *J. Cell Biol.* 131: 583–590.

Johnston, G.C., J.A. Prendergast, and R.A. Singer. 1991. The *Saccharomyces cerevisiae MYO2* gene encodes an essential myosin for vectorial transport of vesicles. *J. Cell Biol.* 113:539–551.

Jungmann, J., and S. Munro. 1998. Multi-protein complexes in the *cis* Golgi of *Saccharomyces cerevisiae* with α-1,6-mannosyltransferase activity. *EMBO (Eur. Mol. Biol. Organ.) J.* 17:423–434.

Karpova, T.S., S.L. Reck-Peterson, N.B. Elkind, M.S. Mooseker, P.J. Novick, and J.A. Cooper. 2000. Role of actin and Myo2p in polarized secretion and growth of *Saccharomyces cerevisiae*. *Mol. Biol. Cell*. 11:1727–1737.

Kuehn, M.J., and R. Schekman. 1997. COPII and secretory cargo capture into transport vesicles. *Curr. Opin. Cell Biol.* 9:477–483.

Kunz, J., U. Schneider, M. Deuter-Reinhard, N.R. Movva, and M.N. Hall. 1993. Target of rapamycin in yeast, TOR2, is an essential phosphatidylinositol kinase homolog required for G1 progression. *Cell*. 73:585–596.

Ladinsky, M.S., D.N. Mastronarde, J.R. McIntosh, K.E. Howell, and L.A. Staehelin. 1999. Golgi structure in three dimensions: functional insights from the normal rat kidney cell. *J. Cell Biol.* 144:1135–1149.

Lawrence, C.W. 1991. Classical mutagenesis techniques. *Methods Enzymol.* 194:273–281.

Lew, D.J., T. Weinert, and J.R. Pringle. 1997. Cell cycle control in *Saccharomyces cerevisiae*. *In* The Molecular and Cellular Biology of the Yeast *Saccharomyces*. Vol. 3. J.R. Pringle, J.R. Broach, and E.W. Jones, editors. Cold Spring Harbor Laboratory Press, Cold Spring Harbor, NY. 607–695.

Lewis, M.J., B.J. Nichols, C. Prescianotto-Baschong, H. Riezman, and H.R.B. Pelham. 2000. Specific retrieval of the exocytic SNARE Snc1p from early yeast endosomes. *Mol. Biol. Cell*. 11:23–38.

Lillie, S.H., and S.S. Brown. 1994. Immunofluorescence localization of the unconventional myosin, Myo2p, and the putative kinesin-related protein, Smy1p, to the same regions of polarized growth in *Saccharomyces cerevisiae*. *J. Cell Biol.* 125:825–842.

Long, R.M., R.H. Singer, X. Meng, I. Gonzalez, K. Nasmyth, and R.P. Jansen. 1997. Mating type switching in yeast controlled by asymmetric localization of *ASH1* mRNA. *Science*. 277:383–387.

Loukin, S., and C. Kung. 1995. Manganese effectively supports yeast cell cycle progression in place of calcium. *J. Cell Biol.* 131:1025–1037.

Lowe, M., N. Nakamura, and G. Warren. 1998. Golgi division and membrane traffic. *Trends Cell Biol.* 8:40–44.

Lussier, M., A.M. Sdicu, T. Ketela, and H. Bussey. 1995. Localization and targeting of the *Saccharomyces cerevisiae* Kre2p/Mnt1p α1,2-mannosyltransferase to a medial-Golgi compartment. *J. Cell Biol.* 131:913–927.

Mehta, A.D., R.S. Rock, M. Rief, J.A. Spudich, M.S. Mooseker, and R.E. Cheney. 1999. Myosin-V is a processive actin-based motor. *Nature*. 400:590–593.

Morin-Ganet, M.-N., A. Rambourg, S.B. Deitz, A. Franzusoff, and F. Képès. 2000. Morphogenesis and dynamics of the yeast Golgi apparatus. *Traffic*. 1:56–68.

Oprins, A., R. Duden, T.E. Kreis, H.J. Geuze, and J.W. Slot. 1993. β-COP localizes mainly to the *cis*-Golgi side in exocrine pancreas. *J. Cell Biol.* 121:49–59.

Orci, L., M. Stamnes, M. Ravazzola, M. Amherdt, A. Perrelet, T.H. Söllner, and J.E. Rothman. 1997. Bidirectional transport by distinct populations of COPI-coated vesicles. *Cell*. 90:335–349.

Osborne, B.I., and L. Guarente. 1989. Mutational analysis of a yeast transcriptional terminator. *Proc. Natl. Acad. Sci. USA*. 86:4097–4101.

Paidhungat, M., and S. Garrett. 1998a. Cdc1 and the vacuole coordinately regulate Mn^{2+} homeostasis in the yeast *Saccharomyces cerevisiae*. *Genetics*. 148: 1787–1798.

Paidhungat, M., and S. Garrett. 1998b. Cdc1 is required for growth and Mn^{2+} regulation in *Saccharomyces cerevisiae*. *Genetics*. 148:1777–1786.
Pelham, H. 1995. Sorting and retrieval between the endoplasmic reticulum and Golgi apparatus. *Curr. Opin. Cell Biol.* 7:530–535.
Pelham, H.R.B. 1998. Getting through the Golgi complex. *Trends Cell Biol.* 8:45–49.
Preuss, D., J. Mulholland, C.A. Kaiser, P. Orlean, C. Albright, M.D. Rose, P.W. Robbins, and D. Botstein. 1991. Structure of the yeast endoplasmic reticulum: localization of ER proteins using immunofluorescence and immunoelectron microscopy. *Yeast*. 7:891–911.
Preuss, D., J. Mulholland, A. Franzusoff, N. Segev, and D. Botstein. 1992. Characterization of the *Saccharomyces* Golgi complex through the cell cycle by immunoelectron microscopy. *Mol. Biol. Cell*. 3:789–803.
Pringle, J.R., A.E.M. Adams, D.G. Drubin, and B.K. Haarer. 1991. Immunofluorescence methods for yeast. *Methods Enzymol.* 194:565–602.
Pruyne, D., and A. Bretscher. 2000. Polarization of cell growth in yeast. II. The role of the cortical actin cytoskeleton. *J. Cell Sci.* 113:571–585.
Pryer, N.K., N.R. Salama, R. Schekman, and C.A. Kaiser. 1993. Cytosolic Sec13p complex is required for vesicle formation from the endoplasmic reticulum in vitro. *J. Cell Biol.* 120:865–875.
Reck-Peterson, S., P.J. Novick, and M.S. Mooseker. 1999. The tail of a yeast class V myosin, Myo2p, functions as a localization domain. *Mol. Biol. Cell*. 10:1001–1017.
Redding, K., C. Holcomb, and R.S. Fuller. 1991. Immunolocalization of Kex2 protease identifies a putative late Golgi compartment in the yeast *Saccharomyces cerevisiae*. *J. Cell Biol.* 113:527–538.
Rose, M.D., P. Novick, J.H. Thomas, D. Botstein, and G.R. Fink. 1987. A *Saccharomyces cerevisiae* genomic plasmid bank based on a centromere-containing shuttle vector. *Gene*. 60:237–243.
Rossanese, O.W., J. Soderholm, B.J. Bevis, I.B. Sears, J. O'Connor, E.K. Williamson, and B.S. Glick. 1999. Golgi structure correlates with transitional endoplasmic reticulum organization in *Pichia pastoris* and *Saccharomyces cerevisiae*. *J. Cell Biol.* 145:69–81.
Rothstein, R. 1991. Targeting, disruption, replacement, and allele rescue: integrative DNA transformation in yeast. *Methods Enzymol.* 194:281–301.
Santos, B., and M. Snyder. 1997. Targeting of chitin synthase 3 to polarized growth sites in yeast requires Chs5p and Myo2p. *J. Cell Biol.* 136:95–110.
Schott, D., J. Ho, D. Pruyne, and A. Bretscher. 1999. The COOH-terminal domain of Myo2p, a yeast myosin V, has a direct role in secretory vesicle targeting. *J. Cell Biol.* 147:791–807.
Segev, N., J. Mulholland, and D. Botstein. 1988. The yeast GTP-binding YPT1 protein and a mammalian counterpart are associated with the secretion machinery. *Cell*. 52:915–924.
Séron, K., V. Tieaho, C. Prescianotto-Baschong, T. Aust, M.-O. Blondel, P. Guillaud, G. Devilliers, O.W. Rossanese, B.S. Glick, H. Riezman, et al. 1998. A yeast t-SNARE involved in endocytosis. *Mol. Biol. Cell*. 9:2873–2889.
Simon, V.R., S.L. Karmon, and L.A. Pon. 1997. Mitochondrial inheritance: cell cycle and actin cable dependence of polarized mitochondrial movements in *Saccharomyces cerevisiae*. *Cell Motil. Cytoskeleton*. 37:199–210.
Siniossoglou, S., S.Y. Peak-Chew, and H.R. Pelham. 2000. Ric1p and Rgp1p form a complex that catalyses nucleotide exchange on Ypt6p. *EMBO (Eur. Mol. Biol. Organ.) J.* 19:4885–4894.
Smith, M.G., V.R. Simon, H. O'Sullivan, and L.A. Pon. 1995. Organelle-cytoskeletal interactions: actin mutations inhibit meiosis-dependent mitochondrial rearrangement in the budding yeast Saccharomyces cerevisiae. *Mol. Biol. Cell*. 6:1381–1396.
Sone, T., and A.J.F. Griffiths. 1999. The *frost* gene of *Neurospora crassa* is a homolog of yeast *cdc1* and affects hyphal branching via manganese homeostasis. *Fungal Genet. Biol.* 28:227–237.
Sprague, G.F., Jr., and J.W. Thorner. 1992. Pheromone response and signal transduction during the mating process of *Saccharomyces cerevisiae*. *In* The Molecular and Cellular Biology of the Yeast *Saccharomyces*. Vol. 2. E.W. Jones, J.R. Pringle, and J.R. Broach, editors. Cold Spring Harbor Laboratory Press, Cold Spring Harbor, NY. 657–744.
Takizawa, P.A., A. Sil, J.R. Swedlow, I. Herskowitz, and R.D. Vale. 1997. Actin-dependent localization of an RNA encoding a cell-fate determinant in yeast. *Nature*. 389:90–93.
Thyberg, J., and S. Moskalewski. 1998. Partitioning of cytoplasmic organelles during mitosis with special reference to the Golgi complex. *Microsc. Res. Tech.* 40:354–368.
Wertman, K.F., D.G. Drubin, and D. Botstein. 1992. Systematic mutational analysis of the yeast *ACT1* gene. *Genetics*. 132:337–350.
Whitney, J.A., M. Gomez, D. Sheff, T.E. Kreis, and I. Mellman. 1995. Cytoplasmic coat proteins involved in endosome function. *Cell*. 83:703–713.
Wooding, S., and H.R.B. Pelham. 1998. The dynamics of Golgi protein traffic visualized in living yeast cells. *Mol. Biol. Cell*. 9:2667–2680.
Wu, X., G. Jung, and J.A.I. Hammer. 2000. Functions of unconventional myosins. *Curr. Opin. Cell Biol.* 12:42–51.
Yaffe, M.P. 1991. Organelle inheritance in the yeast cell cycle. *Trends Cell Biol.* 1:160–164.
Yaffe, M.P. 1999. The machinery of mitochondrial inheritance and behavior. *Science*. 283:1493–1497.
Zaal, K.J., C.L. Smith, R.S. Polishchuk, N. Altan, N.B. Cole, J. Ellenberg, K. Hirschberg, J.F. Presley, T.H. Roberts, E. Siggia, et al. 1999. Golgi membranes are absorbed into and reemerge from the ER during mitosis. *Cell*. 99: 589–601.
Zheng, N., and L.M. Gierasch. 1996. Signal sequences: the same yet different. *Cell*. 86:849–852.